Deposition, Erosion and Hydrocarbon Source Potential of the Oligocene Eggerding Formation (Molasse Basin, Austria)

Reinhard F. SACHSENHOFER[1)*)], Birgit LEITNER[1)], Hans-Gert LINZER[2)], Achim BECHTEL[1)],

Stjepan ĆORIĆ[3)], Reinhard GRATZER[1)], Doris REISCHENBACHER[1)] & Ali SOLIMAN[4)]

[1)] Department Applied Geosciences and Geophysics, Montanuniversität, Peter-Tunner-Str. 5, A-8700 Leoben, Austria;

[2)] Rohöl-Aufsuchungs AG, Schwarzenbergplatz 16, A-1015 Vienna, Austria;

[3)] Geological Survey of Austria, Neulinggasse 38, A-1030 Vienna, Austria;

[4)] Institute of Earth Sciences, Karl-Franzens-Universität Graz, Heinrichstr. 26, A-8010 Graz, Austria;

[*)] Corresponding author, reinhard.sachsenhofer@unileoben.ac.at

Abstract

The Eggerding Formation, typically about 45 m thick, forms part of the deep marine Oligocene succession in the Molasse Basin, which comprises from bottom to top the Schöneck (formerly "Fish Shale"), Dynow ("Bright Marlstone"), Eggerding ("Banded Marl") and Zupfing formations ("Rupelian Marl"). The Eggerding Formation and the lower part of the Zupfing Formation have been studied using core and cuttings samples and a multidisciplinary approach involving core description, geochemistry, palynology and nanno-paleontology.

The Dynow Formation and the lower part of the Eggerding Formation were deposited during nannoplankton zone NP23 (Martini, 1971). The transition between the Dynow and Eggerding formations is characterized by a gradual decrease in carbonate contents. The Eggerding Formation deposited in near-shore environments contains several sand layers. In contrast, the Eggerding Formation deposited along the northern slope is generally poor in sand. Its lower part consists of dark grey laminated shaly marlstone with white bands rich in coccolithophorides. TOC contents are about 5 %. The upper part of the Eggerding Formation consists of a homogenous sequence of marly shale and includes in average 1.6 % TOC.

Oxygen deficient conditions prevailed during deposition of the Eggerding Formation. Marine palynomorphs are present in all samples from the Eggerding Formation, but calcareous nannoplankton is restricted to its lower part. Salinity variations are recorded in rocks of the lower part of the Eggerding Formation. The environment during deposition of its upper part was more stable. Log signatures, which are comparable over tens of kilometres, provide evidence for the lateral continuity of the Eggerding Formation deposited on the upper slope.

Slope instabilities are indicated by slumps and extensive submarine slides. Sliding reached a maximum at the transition from the Eggerding to the Zupfing Formation, when locally a succession up to 70 m thick was removed from the northern slope. The slided material was redeposited either on the northern slope or at the base of the slope.

The Eggerding Formation is overlain by the Zupfing Formation (NP24), consisting of clay marl up to 450 m thick. Oxygen-depleted conditions continued during deposition of the Zupfing Formation, but only the lowermost few meters of the Zupfing Formation ("Transition Zone") are rich in organic matter (1.5 % TOC).

Whereas the lower part of the Eggerding Formation (TOC 1.9-6.0 %; HI up to 600 mg HC/g TOC) holds a very good source potential for oil (and gas), its upper part and the Transition Zone (TOC: ~1.5 %; "true" HI 500-600 mg HC/g TOC) are characterized by a good potential. Biomarker data suggest that the latter contributed significantly to the Molasse oils. In contrast, the contribution of the Dynow Formation and the lower Eggerding Formation was minor.

Die ca. 45 m mächtige Eggerding-Formation ist Teil der tief marinen oligozänen Abfolge des Molassebeckens. Diese umfasst vom Liegenden zum Hangenden Schöneck- (früher „Fischschiefer"), Dynow- („Heller Mergelkalk"), Eggerding- („Bändermergel") und Zupfing-Formation („Rupel Tonmergel"). Die Eggerding-Formation und der tiefere Anteil der Zupfing-Formation wurden anhand von Kern- und Bohrkleinproben untersucht. Die Untersuchungsverfahren inkludierten Kernbeschreibung, Geochemie, Palynologie und Nannopaläontologie.

Die Dynow-Formation und der untere Anteil der Zupfing-Formation wurden während der Nannoplankton-Zone NP23 (Martini, 1971) abgelagert. Der Übergang von der Dynow- zur Eggerding-Formation wird durch eine graduelle Abnahme des Karbonatgehaltes charakterisiert. Eggerding-Formation, die in einem küstennahen Bereich abgelagert wurde, beinhaltet zahlreiche Sandsteinlagen. Im Gegensatz dazu ist jene, die am nördlichen Hang des Molassebeckens abgelagert wurde, generell arm an Sandstein. Der untere Teil der Eggerding-Formation weist dunkelgraue, laminierte tonige Mergelsteine mit weißen Bändern, die reich an Coccolithophoriden sind, auf. Der Gehalt an organischem Kohlenstoff (TOC) beträgt ca. 5 %. Der obere Teil der Eggerding-Formation besteht aus einer gleichförmigen Abfolge von mergeligen Tonsteinen und beinhaltet durchschnittlich ca. 1.6 % TOC.

Sauerstoffreduzierte Bedingungen herrschten während der Ablagerung der Eggerding-Formation vor. Marine Palynomorphen sind in allen Proben der Eggerding-Formation präsent. Kalkiges Nannoplankton ist dagegen auf deren unteren Teil beschränkt. Während

Reinhard F. SACHSENHOFER, Birgit LEITNER, Hans-Gert LINZER, Achim BECHTEL, Stjepan ĆORIĆ, Reinhard GRATZER, Doris REISCHENBACHER & Ali SOLIMAN

die Umweltbedingungen zur Zeit der Ablagerung des oberen Teils der Eggerding-Formation relativ stabil waren, variierte die Salinität während der Ablagerung des unteren Teils. Logmuster, die über Zehnerkilometer verfolgt werden können, belegen die hohe laterale Kontinuität der Eggerding-Formation im Bereich des oberen Hanges.

Hanginstabilitäten werden durch Rutschfalten und ausgedehnte submarine Rutschungen angezeigt. Diese erreichten an der Grenze Eggerding-/Zupfing-Formation ein Maximum, als bis zu 70 m mächtige Sedimentstapel am nördlichen Hang abgerutscht sind. Das umgelagerte Material wurde am Hang oder an dessen Basis abgelagert.

Die Eggerding-Formation wird von bis zu 450 m mächtigen tonigen Mergeln der Zupfing-Formation (NP24) überlagert. Sauerstoffreduzierte Bedingungen dauerten während der Ablagerung der Zupfing-Formation an, aber nur deren unterste Meter („Übergangszone") sind reich an organischem Material (1.5 % TOC).

Der untere Teil der Eggerding-Formation (TOC 1.9-6.0 %; HI bis zu 600 mg HC/g TOC) besitzt ein sehr gutes Muttergesteinspotential für Öl (und Gas). Der obere Teil der Eggerding-Formation und die Übergangszone (TOC: ~1.5 %; "wahrer" HI 500-600 mg HC/g TOC) werden dagegen durch ein gutes Muttergesteinspotential charakterisiert. Biomarkerdaten zeigen, dass die letzteren signifikant zur Bildung der Molasseöle beigetragen haben, der Beitrag der Dynow-Formation und der unteren Eggerding-Formation aber gering war.

1. Introduction

The fine-grained Lower Oligocene succession in the Molasse Basin comprises from bottom to top: Schöneck Formation (formerly "Fish Shale"), Dynow Formation ("Bright Marlstone"), Eggerding Formation ("Banded Marl") and Zupfing Formation ("Rupelian Marl"; Wagner, 1998). Detailed studies of the depositional environment and hydrocarbon source potential of the Schöneck and Dynow formations were published recently (Schulz et al., 2002, 2004, 2005; Sachsenhofer and Schulz, 2006). In contrast little information is available on the Eggerding and Zupfing formations.

The Schöneck Formation is regarded as the main source rock for oil and thermogenic gas in the Molasse Basin. Schmidt and Erdogan (1996) recognized that beside the Schöneck Formation, the Eggerding Formation has some additional, but subordinate source rock potential. Based on high TOC contents (< 4 %) at the base of the Eggerding Formation, Sachsenhofer and Schulz (2006) speculated that the source potential of the Eggerding Formation could be underestimated.

The objective of the present study is to investigate the depositional environment and hydrocarbon source potential of the Eggerding Formation (and the lowermost part of the Zupfing Formation) in the Austrian part of the Molasse Basin using core and cuttings samples and a multi-disciplinary approach involving sedimentology, geochemistry, palynology and nannopaleontology. Log and seismic data are used to characterize an early Oligocene erosion event, which is indicated by major lateral thickness variations (Sachsenhofer and Schulz, 2006).

2. Geological Setting

The Molasse Basin extends along the northern margin of the Alps from Geneva to Vienna (Fig. 1). It represents a foreland basin, which developed since Eocene times in response to loading of the southern margin of the European plate after the Alpine orogeny (Bachmann et al., 1987; Genser et al., 2007). In the Austrian sector, the basin is delineated to the north by the outcropping basement of the Bohemian Massif, whereas the southern part of the basin is overthrust by the Alpine nappes.

Overlying crystalline basement or Mesozoic rocks, the oldest sediments marking the initial evolution of the Molasse Basin are of Late Eocene age (Fig. 2). The sedimentary succession is characterized by non marine and shallow marine clastic deposits and carbonate rocks (Rasser and Piller, 2004). During the early Oligocene, the Molasse Basin deepened and widened abruptly (Sissingh, 1997) resulting in the deposition of deepwater deposits:

The Schöneck Formation, typically about 10 to 20 m thick, consists of organic-rich marls (units A, B) and shales (unit C; Schulz et al., 2002, Sachsenhofer and Schulz, 2006). The water depth during deposition of the Schöneck Formation increased up to 600 m (Dohmann, 1991).

The Dynow Formation, 5 to 15 m thick, follows above a sharp boundary. It consists of an intercalation of (marly) limestones deposited during algal blooms and organic-rich marls.

The Eggerding Formation is composed of dark gray laminated pelites. Drill holes along the northern margin of the Molasse Basin indicate a near-shore environment with abundant
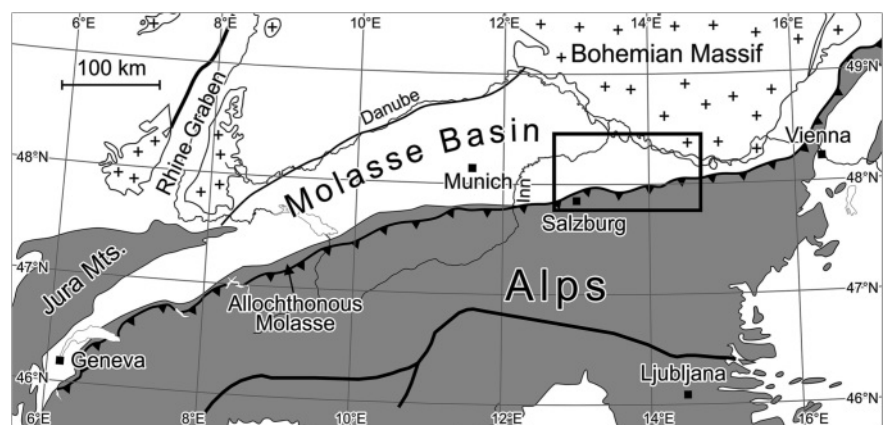

FIGURE 1: Sketch map of the Molasse Basin extending from Geneva to Vienna. The black rectangle marks the study area.

sandstone layers. Some of these sandstones carry heavy biodegraded oil at shallow positions (Brix and Schultz, 1993). The thickness of the Eggerding Formation varies typically in the range of 35 to 45 m, but is significantly lower in areas with submarine erosion (Sachsenhofer and Schulz, 2006; Fig. 3). Obviously erosion was especially effective west of the Lindach Fault in the Ried-Schwanenstadt, Puchkirchen, and Braunau blocks (Fig. 3). These tectonic blocks are separated by Mesozoic faults, which were reactivated during Paleogene time (Wagner, 1998). Sachsenhofer and Schulz (2006), therefore, speculated that gravity-induced movements were triggered by earthquakes.

The Eggerding Formation is overlain by the Zupfing Formation, which is up to 450 m thick. It consists mainly of dark gray hemipelagites and distal turbidities from the south. They are intercalated with slumps, slides and turbidites derived from the northern slope. Nannofossil limestone layers occur in the lower part of the section (Wagner, 1996, 1998).
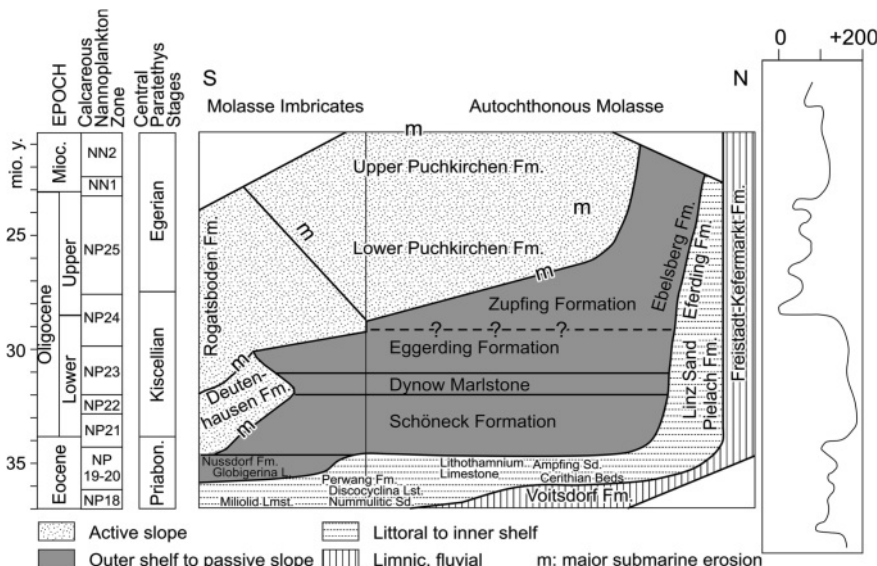
According to sequence stratigraphic analysis (Jin et al., 1995; Zweigel, 1998), shallow marine Eocene sediments, and deep marine Lower Oligocene deposits form a transgressive systems tract. The Zupfing Formation represents very distal, basinal highstand deposits (Zweigel 1998). A major sea level fall (200 m) occurred at the boundary between Lower and Upper Oligocene (e.g. Haq et al., 1987).

Whereas a deltaic complex filled the western part of the Molasse Basin, deep marine conditions with water depths exceeding 1000 m (Rögl et al., 1979) persisted during Late Oligocene to Early Miocene times east of the river Inn. The deepest parts of the foredeep were filled by coarse-grained sediments of an axial channel belt and margin slope fans (Puchkirchen Formation; Egerian to Early Eggenburgian; Hubbard et al., 2005; de Ruig and Hubbard, 2006; Covault et al., 2009).

After a prominent early Miocene submarine erosion event, the marine Hall (Eggenburgian) and Innviertel (Ottnangian) groups were deposited recording a gradational transition to shallow-water sedimentation. Brackish-water sediments were deposited during the upper Ottnangian and coal-bearing freshwater sediments prevailed during Badenian to Pannonian times.

3. Materials and Data Set

Hundreds of wells drilled the Eggerding Formation in the Molasse Basin of Upper Austria, but the core coverage is generally poor. Cores representing the whole Eggerding Formation are available only from one well in the Eggerding area (Egdg; see Fig. 3). This shallow well provides information on the Eggerding Formation deposited in a near-shore environment and is represented in this study by 15 core samples. The lowermost 4 m of the Eggerding Formation deposited on the upper paleoslope were investigated using 13 core samples from well Oberschauersberg (Osch). This well has been selected, because information on the Schöneck and Dynow formations is already available (Schulz et al., 2002; 2004). The upper part of the Eggerding Formation and the lower part of the Zupfing Formation have been studied using cores from wells in the Voitsdorf (V; 14 samples) and Puchkirchen fields (P; 44 samples). In order to investigate a continuous profile from the Eocene limestones to the Zupfing Formation in an upper slope setting, 94 cuttings samples

Figure 2: Stratigraphic chart of Paleogene rocks in the Austrian Molasse Basin (modified after Wagner 1998). m – submarine erosion.
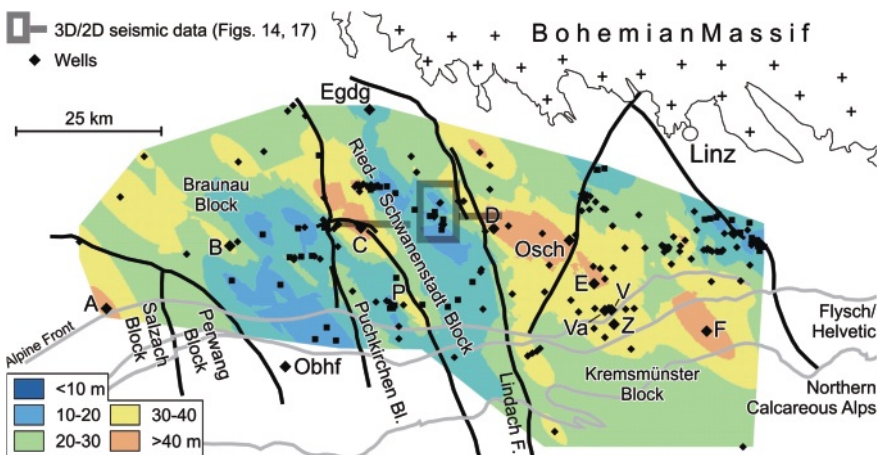

Figure 3: Thickness distribution of the Eggerding Formation (Sachsenhofer and Schulz, 2006). The map is based on information from wells indicated in the map. Wells discussed in the text are labeled.

from well Z have been added in the study. With the exception of well Osch and the Zupfing Formation in well Z, the sampling interval was about 1 m. The investigated intervals are shown together with wire-line logs in Fig. 4.

Gamma Ray (GR) and Sonic logs (DT) from 92 boreholes distributed across the study area were used for well correlations. A 3D seismic cube covering 66 km² in the Trattnach area was used to characterize the seismic facies of the Eggerding Formation and to map its thickness distribution.

4. Methods

All samples were analyzed for total sulphur (S), total carbon (TC), and total organic carbon contents (TOC) using a Leco CS-300 analyzer. TC and TOC contents were used to calculate calcite equivalent percentages (=8.34 *[TC-TOC]).

RockEval pyrolysis (Espitalié et al., 1977) was carried out using a Rock-Eval 2+ instrument. By this method, the amount of hydrocarbons (mg HC/g rock) present in the rock sample (S1) and released from kerogen during gradual heating (S2) was determined and used to calculate the Genetic Potential (S1+S2) and the Hydrogen Index (HI = S2*100/TOC). Tmax

was measured as a maturation indicator.

Calcareous nannoplankton from 38 core samples from the Eggerding and Zupfing formations from boreholes Osch, P and Egdg was studied semi-quantitatively (see Sachsenhofer et al., 2009 for the applied techniques).

Palynological investigations were performed on 21 core samples from the same wells. 20 g of each sample have been prepared following established procedures (e.g. Tyson, 1995; Batten, 1996). The residue was split into two fractions used for palynofacies analysis and dinoflagellate cyst taxonomy. For the earlier, the residue was sieved at 10 μm (Batten and Stead, 2005) and a kerogen slide was prepared. A total of 500 organic particles was classified according to (1) amorphous organic matter (AOM), (2) terrestrial elements (opaque and translucent phytoclasts, non-saccate and bisaccate sporomorphs), and (3) marine palynomorphs (dinocysts, acritarchs, foraminiferal test linings) (e.g. Pittet and Gorin, 1997). The second residue fraction was treated for c. 1 min. in ultrasonic bath, sieved at 20 μm, slightly oxidized with diluted HNO_3, and stained with Safranin "O". Two slides from selected samples were prepared and scanned microscopically for dinoflagellates. The di-
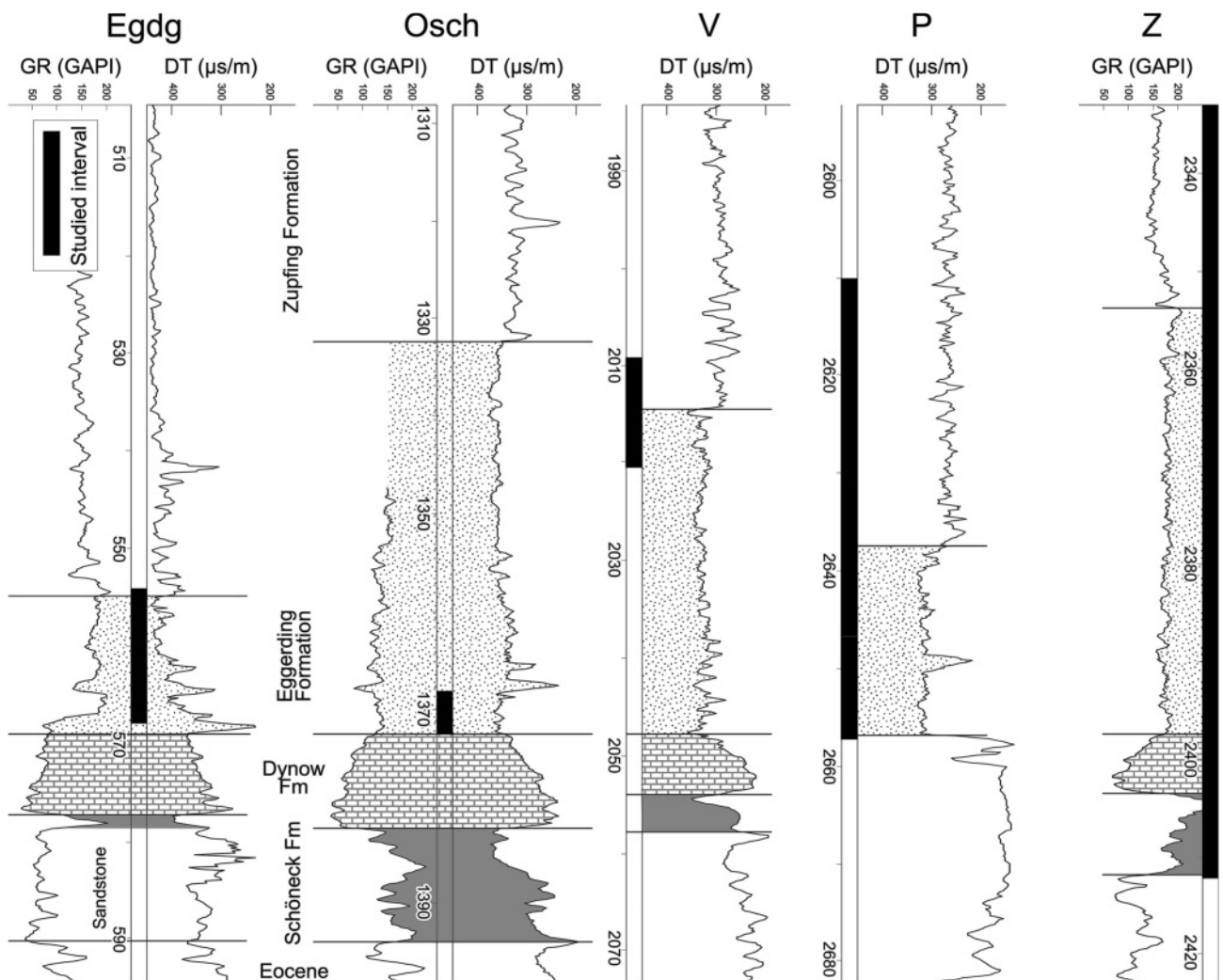

Figure 4: Logs of investigated wells; black bars show position of investigated intervals. GR – Gamma Ray, GAPI – American Petroleum Institute gamma units; DT – Sonic log.

noflagellate cyst nomenclature generally follows that of Fensome et al. (2008).

For mineral and maceral analysis thin sections and polished blocks of selected core samples were prepared and studied using Leica microscopes.

For the decomposition of calcite for mass spectrometric analysis, weighed portions of the samples were evacuated and flooded with He using the Gasbench II (Thermo Scientific). Carbon and oxygen isotope measurements were perfomed by addition of 100 % H_3PO_4 to the samples heated at 70°C using a GC PAL on-line system and subsequent analysis of ^{13}C and ^{18}O using a Finnigan DELTA-V isotope ratio mass spectrometer. The results are reported relative to the Pee Dee Belemnite (PDB) standard for both $\delta^{13}C$ and $\delta^{18}O$. The reproducibility was better than 0.2‰.

Five samples from well Osch and seven samples from P have been selected for biomarker analysis. See Sachsenhofer et al. (2009) for the applied analytical techniques and the used instrumentation.

5. Results

5.1 Sedimentology, Bulk geochemical parameters, Palynofacies, Calcareous Nannoplankton

5.1.1 Eggerding

Eggerding Formation, about 14 m thick, has been drilled in well Eggerding. At this locality the contact between the Dynow and Eggerding formations is erosive. The lowermost 1.45 m of
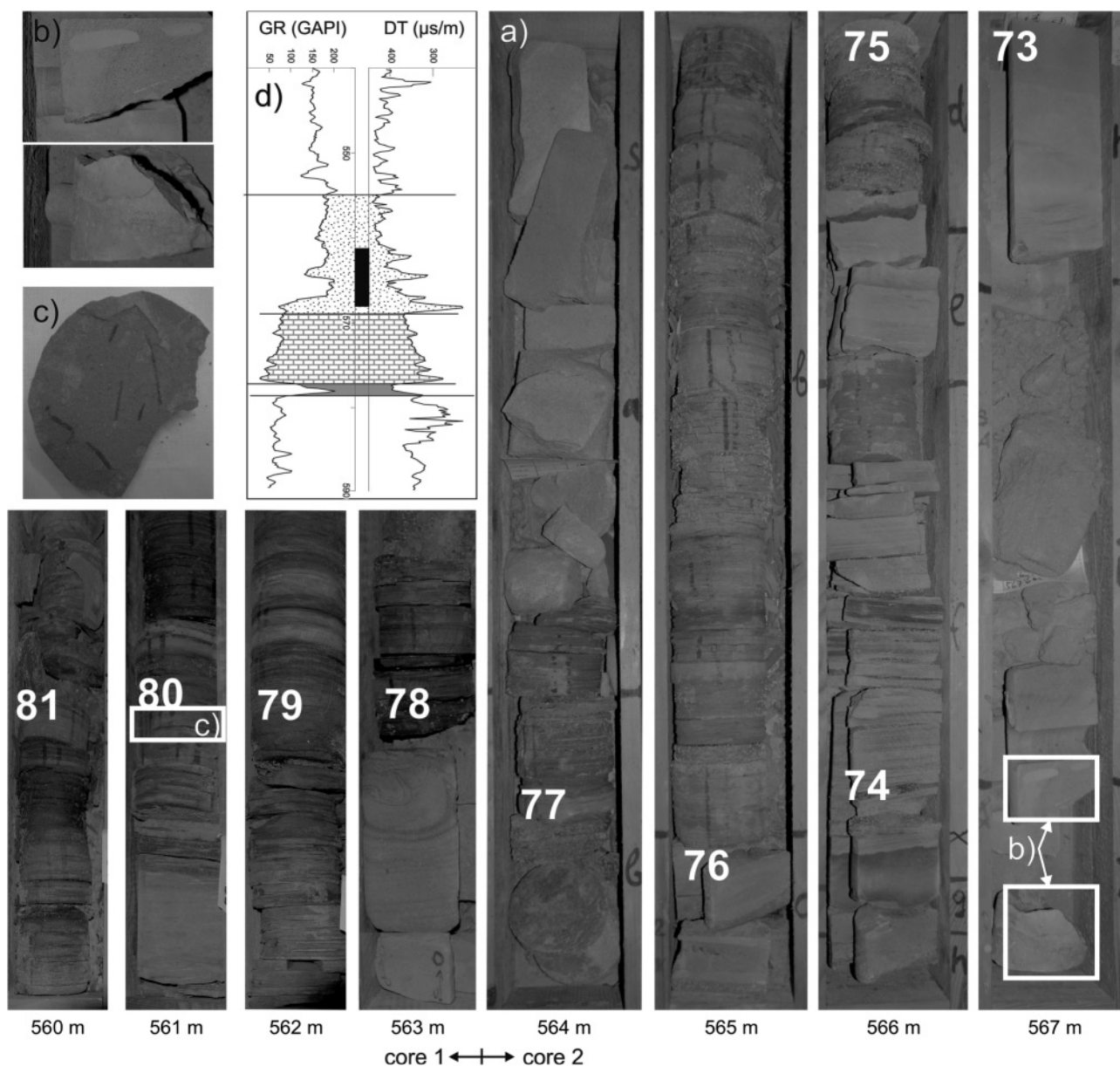

Figure 5: a) Section of drill cores 1 and 2 from well Eggerding recovering the lower, sand-rich part of the Eggerding Formation. 73 to 81 are sample numbers; b) details of the base of the Eggerding Fm., c) plant remains on bedding plane. d) Gamma-ray (GR) and sonic (DT) logs, location of core section shown in a) is indicated by a black bar.

the Eggerding Formation is composed of sandstone which contains clasts of the Dynow Formation, up to 10 cm in diameter, near its base (Fig. 5a, b). The basal sandstone is overlain by pelitic rocks with low carbonate contents (0-5 %) interfingering with sandstone beds. Number and thickness of sandstone layers decrease upwards, but thin laminae with silt and fine-grained sand are also abundant in the pelitic layers. Macroscopic remains of land plants (Fig. 5c) and fish remains occur frequently.

TOC contents of pelitic rocks range from 0.84 to 2.30 %, whereas HI values vary between 105 and 320 mg HC/g TOC (Fig. 6). Relatively low TOC contents occur in silty to sandy samples and result from dilution by detrital minerals. However, the highest TOC content (3.62 %) and the maximum HI value (436 mg HC/g TOC) are recorded in a siltstone to fine-grained sandstone at the top of the basal coarse-grained layer (sample 73; Fig. 5). The high TOC content of this sample results from abundant lamalginite resting in a fluorescing pelitic matrix.

Two of four palynofacies samples (74, 83) contain relatively high amounts of phytoclasts (35-40 %). In contrast, the remaining samples (77, 87) are relatively poor in phytoclasts (<20 %), but rich in AOM (78 %; Fig. 6). Sample 77 contains a very abundant and highly diversified dinoflagellate cyst assemblage. Many Mid Oligocene (Late Rupelian-Early Chattian; e.g. Williams et al., 2004) dinoflagellate cysts such as Wetzeliella articulata Eisenack, 1938, *Wetzeliella gochtii* Costa and Downie, 1976, *Rhombodinium draco* Gocht, 1955, *Enneadocysta pectiniformis* (Gerlach) Stover and Williams, 1995, *Cordosphaeridium cantharellus* (Brosius, 1963) Gocht, 1969, *Distatodinium ellipticum* (Cookson, 1965) Eaton, 1976, *Distatodinium paradoxum* (Brosius, 1963) Eaton, 1976, *Distatodinium scariosum* Liengjarern et al., 1980 and *Deflandrea phosphoritica* Eisenack, 1938 have been recorded (Plate 1). Sample 77 is also very rich in the green algae *Pediastrum*.

The TOC/S ratios range from 0.2 to 1.2 indicating that euxinic conditions (Berner, 1984) prevailed in the near shore environment. Tmax (406°C) and vitrinite reflectance (0.24 %Rr; Table 1) prove very low thermal maturity.

Three fine-grained samples in the interval from 553.65 m to 557.64 m were tested for calcareous nannoplankton but turned out to be barren.

5.1.2 Oberschauersberg

The Eggerding Formation in well Osch is about 40 m thick, but only its lowermost part (4.3 m) has been cored (Fig. 7). Analytical data of this part of the Eggerding Formation are shown together with those from the Schöneck and Dynow formations (after Schulz et al., 2002, 2004) in Fig. 6.

Although the carbonate content decreases significantly across the Dy-now/Eggerding formations boundary in well Osch (Fig. 6), the transition is generally gradual. The lower part of the Eggerding Formation contains dark grey laminated shaly marlstone with white nannoplankton-rich bands (Fig. 7b, c). Because of these thin bands, the Eggerding Formation was formerly termed "banded marl". Fish remains occur in many samples.

Two turbiditic sandstone layers, 12 and 8 cm thick, are present in the cored interval of the Eggerding Formation in well Osch (Fig. 7a, d). The fine to middle grained sandstone is porous and contains land plants and rip up clasts. The presence of even thicker sandstone layers above the studied interval is indicated by the log response (Fig. 4).

The calcite content of the pelitic rocks ranges from 1.3 to 17.0 % (average 9.6 %). TOC contents remain high across the boundary between Dynow and Eggerding formations and vary between 1.9 and 6.0 % (average: 3.2 %). HI values in the Eggerding Formation range from 300 to 580 mg HC/g TOC and are slightly lower than in the underlying Dynow Formation. However, plots of S2 versus TOC (Langford and Blanc-Valleron, 1990) suggest that the "true" HI is about 650 mg HC/g TOC, which is similar to that in the Schöneck and Dynow formations. Tmax (423°C) and vitrinite reflectance (0.31 %Rr; Tab. 1) show that the organic matter is immature.

High HI values agree with palynofacies data of samples 59, 61, 62, 65, 67, 68, 72 (see Fig. 7 for position of samples), which show that the organic matter is very rich in AOM (76-91 %) and poor in phytoclasts (6-17 %; Fig. 6). Two samples (59, 67), after enhanced preparation, have been scanned for their dinoflagellate cysts content. The recovered marine phytoplankton is of low abundance and diversity and includes the Oligocene taxa *Wetzeliella gochtii*, *Wetzeliella articulata*, *Membranophoridium aspinatum* Gerlach, 1961, *Hystrichokolpoma truncatum* Biffi and Manum, 1988, *Glaphyrocysta* spp., *Cordosphaeridium cantharellus*, *Caligodinium amiculum* Drugg, 1970, *Fibrocysta axialis* (Eisenack, 1965) Stover and Evitt, 1978, and *Deflandrea phosphoritica*.

TOC/S ratios (1.1-2.6) are generally below the values characteristic for normal marine environments (Berner, 1984). This fact and the absence of bioturbation indicate oxygen-depleted conditions.

No calcareous nannoplankton was detected in samples 60, 63, 66, 71, and 72. In contrast, apart from common redeposited Cretaceous to Eocene nannofossils, well preserved Oligocene taxa were detected in samples 61, 64, and 68: *Cocco-*

	Depth (m, TVD)	VR (%Rr)	Tmax (°C)	20S/(20S+20R) C$_{29}$-Steranes	22S/(22S+22R) C$_{31}$-Hopanes	Tri-/(Tri- + Mono-) Arom. Steroide
Egdg	553-566	0.24	406			
Osch	1368-1372	0.31	423	0.00-0.07	0.31-0.38	0.07-0.10
V	2008-2021	0.42	428			
Z	2300-2420	0.51	426			
P	2613-2655	0.53	430	0.16-0.30	0.56-0.57	0.58-0.71

TABLE 1: Maturity parameters (TVD – true vertical depth; VR – vitrinite reflectance)

lithus pelagicus (Wallich) Schiller, *Cyclicargolithus floridanus* (Roth & Hay) Bukry, *Reticulofenestra bisecta* (Hay) Roth, *R. lockeri* Müller, *R. stavensis*, *Sphenolithus* cf. *capricornutus* Bukry & Percival, *Reticulofenestra* sp. Sample 68 (1369.17 m) contains the endemic form *Reticulofenestra ornata* Müller, and *Braarudosphaera bigelowii* (Graan & Braarud) Deflandre. The latter form, characteristic for reduced salinity (Bukry, 1974),

was also detected in high percentages in sample 64 (1370.50 m).

5.1.3 Voitsdorf

The upper 7 m of the 35-m-thick Eggerding Formation and the lowermost 8 m of the Zupfing Formation have been cored in well V. The sharp formation boundary is well visible, because cores of the Eggerding Formation are less compact than cores of Zupfing Formation. This is mainly a result of varying carbonate contents (Eggerding Fm.: <10 %; Zupfing Fm: 20-37 %).

The upper part of the Eggerding Formation consists of a uniform succession of marly shale. In contrast to the lower part, it does not show the typical white bands and bedding is not well developed. Fish remains are common. The TOC content of the cored interval of the Eggerding Formation in well V ranges from 1.3 to 2.4 % (average 1.8 %; Fig. 6).

The studied interval of the Zupfing Formation consists of clay marl. Thin carbonaceous layers cause distinct bedding. The TOC content in its lowermost six meters is nearly as high as in the Eggerding Formation (~1.5 %) and decreases only in the uppermost sample to 0.6 %. We term this interval, characterized by relatively high calcite and TOC contents the "Transition Zone". Because of the high calcite content, this Transition Zone forms part of the Zupfing Formation on geophysical logs.

HI ranges from 230 to 380 mg HC/g TOC in the Eggerding Formation and the Transition Zone, and is 140 mg HC/g TOC in the overlying sample of the Zupfing Formation. Average Tmax (428°C) and vitrinite reflectance (0.42 %Rr; Tab. 1) indicate that the organic matter is immature.

TOC/S ratios are very low in all samples (0.2-1.2) argueing for a euxinic depositional environment (Berner, 1984).

5.1.4 Puchkirchen

The entire interval from the Eocene limestones to the Zupfing Formation has been cored in well P. However, log patterns suggest that beside the Schöneck and Dynow formations also the lower part of the Eggerding
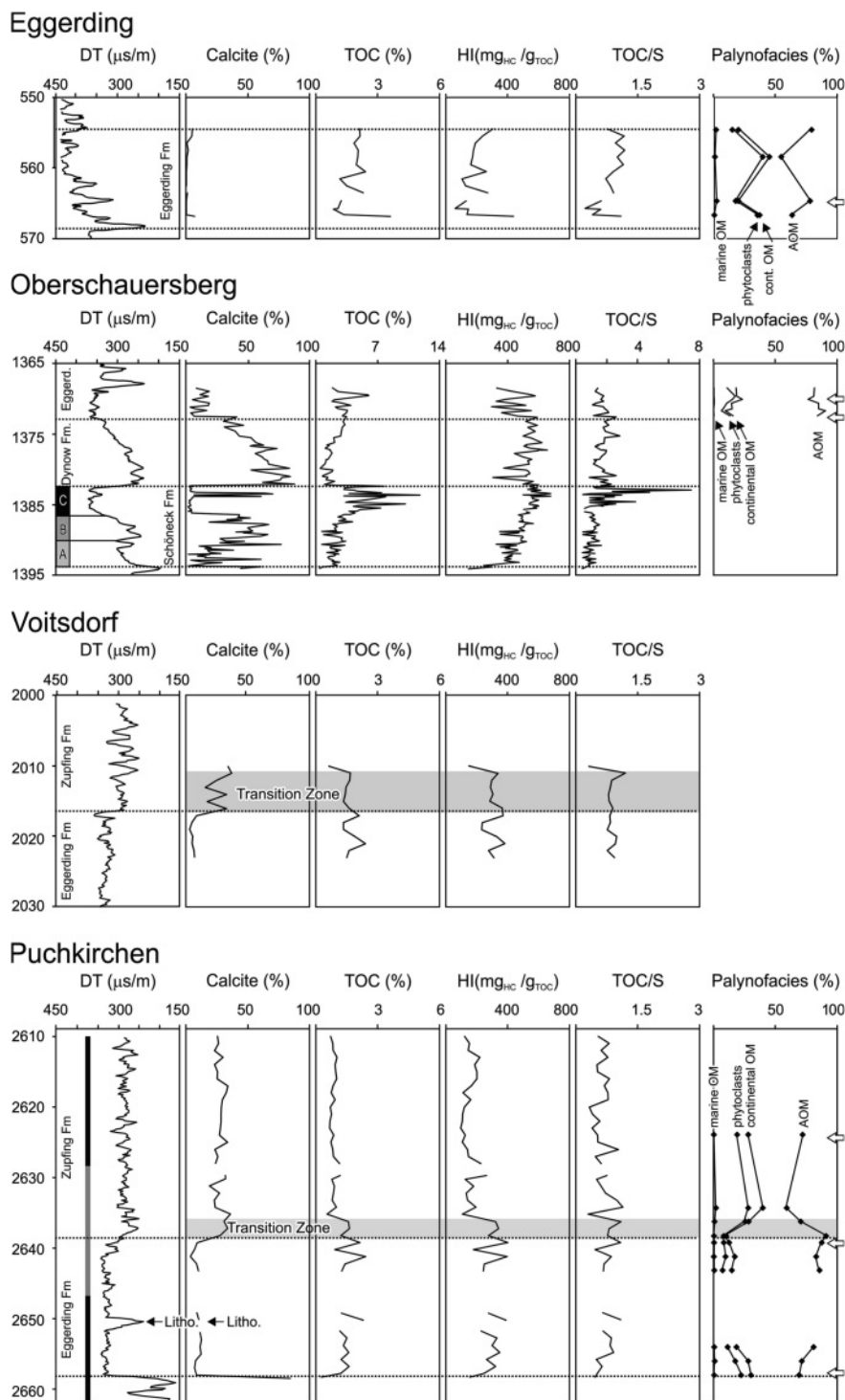

Figure 6: Sonic log (DT), calcite contents, source rock parameters and palynofacies data of the Eggerding Formation and the lower part of the Zupfing Formation in selected wells. Samples used for dinoflagellate taxonomy are indicated by arrows. Data from the Dynow and Schöneck formations in well Oberschauersberg are from Schulz et al. (2002; 2004).

Formation is missing (Fig. 4). Thus, similar to well V, well P provides information on the upper part of the Eggerding Formation and the lower part of the Zupfing Formation (Fig. 4). Moreover, because of incomplete core recovery, the exact depth assignment for samples between 2628 and 2660 m depth is difficult.

The less than 20-m-thick Eggerding Formation in well P is composed primarily of dark grey, partly laminated, marly shales (calcite: 3-12 %) with 1.0 to 2.4 % (1.5 %) TOC. Fish scales are

frequently observed. The lowermost 30 cm contain clasts of Eocene limestone, up to 7 cm in diameter. Reworked limestone, 11 cm thick, also occurs in core material 6.3 m above the base of the Eggerding Formation. Despite the uncertain exact depth, it is reasonable to assume, that it is related to the spike in the DT log at about 2650 m depth.

The Transition Zone in well P is only 3 m thick (calcite: 28-34 %; TOC: 1.2-1.5 %). TOC contents in the Zupfing Formation
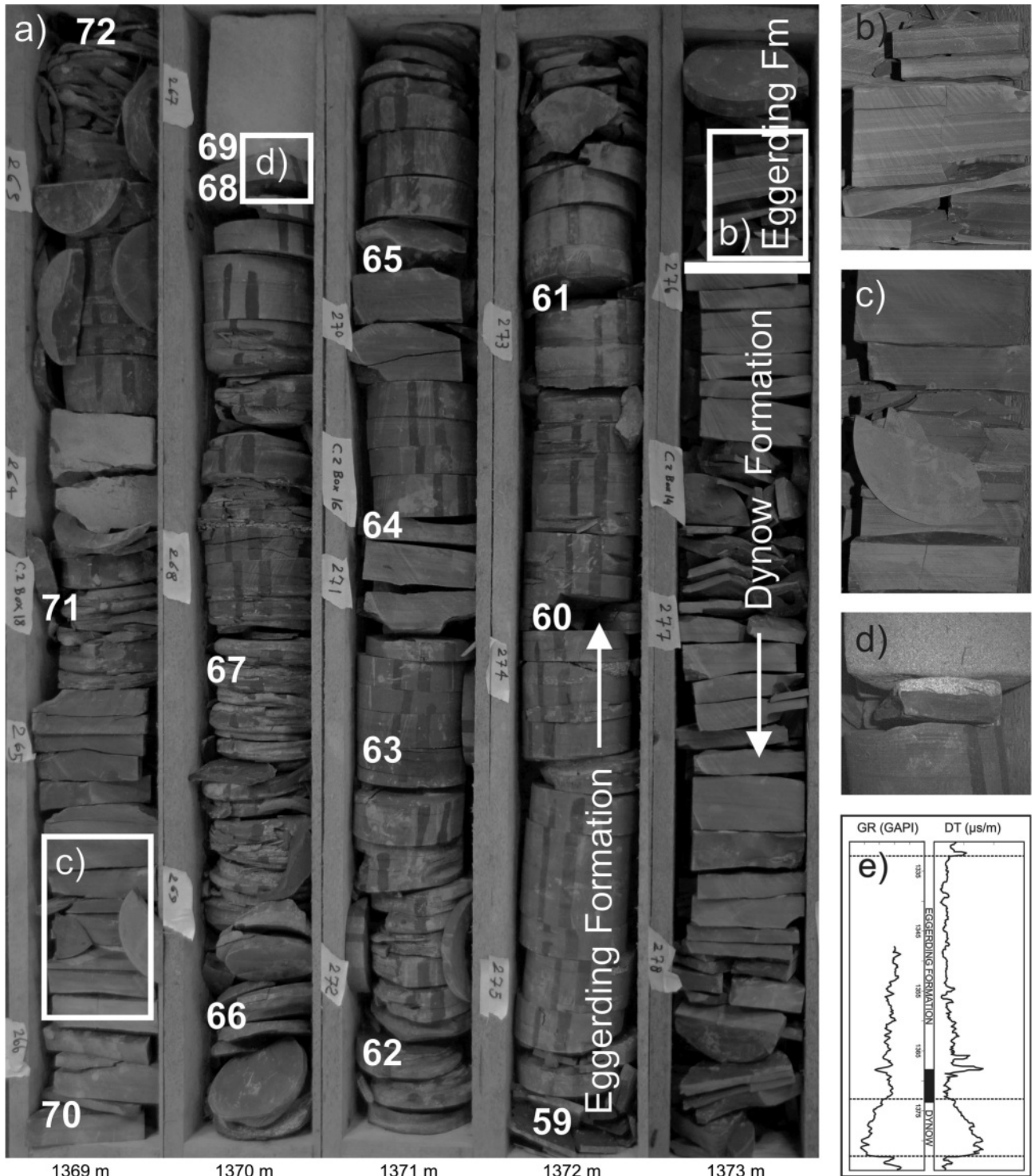

FIGURE 7: a) Section of drill core from well Osch. 59 to 72 are sample numbers; b-c) details of banded marl; d) base of turbiditic sandstone. e) Gamma-ray (GR) and sonic (DT) logs, location of core section shown in a) is indicated by a black bar.

above the Transition Zone vary from 0.5 to 1.2 % (0.8 %). In general, sediments from the Transition Zone show a higher degree of lamination than the overlying sediments. Both, the Transition Zone and their overburden contain abundant planktonic foraminifers.

HI values range from 200 to 400 mg HC/g TOC in the Eggerding Formation and the Transition Zone, and from 100 to 250 mg HC/g TOC in the overlying sediments of the Zupfing Formation. However, plots of S2 versus TOC (Langford and Blanc-Valleron, 1990) suggest that this difference is mainly due to a mineral matrix effect and that there is no significant difference between the "true" HI (~525 mg HC/g TOC) of organic matter in both formations. Tmax (430°C) and vitrinite reflectance (0.53 %Rr) in the deep well P are higher than in any other studied well (Tab. 1). Similar to well V, TOC/S ratios (0.3-1.1) indicate euxinic conditions.

Palynofacies data from ten samples show that AOM is the dominant palynodebris in all samples (Fig. 6). Its percentage increases upwards within the Eggerding Formation from 69 to 87 %, reaches a maximum (91 %) just above the base of the Zupfing Formation, and decreases to a minimum (58 %) in sediments overlying the Transition Zone. The stratigraphically highest sample indicates another upward increase in AOM abundance. The amount of terrestrial organic matter (sporomorphs: 1-12 %; phytoclasts: 7-28 %) shows an opposite trend. The amount of marine organic matter is low (<2 %). Dinoflagellate cyst assemblages from three selected samples (Eggerding Fm.: 2, 15; Zupfing Fm.: 30) are relatively high in terms of abundance and diversity. The assemblage is quite rich in *Caligodinium amiculum*, *Chiropteridium galea* (Maier) Sarjeant, 1983, *Chiropteridium lobospinosum* Gocht, 1960,

Cleistosphaeridium spp., *Cordosphaeridium cantharellus*, *Deflandrea phosphoritica*, *Distatodinium paradoxum*, *Distatodinium biffii* Brinkhuis et al., 1992, *Distatodinium ellipticum*, *Lejeunecysta* spp., *Rhombodinium draco*, *Spiniferites/Achomosphaera* spp., *Selenopemphix* spp. *Wetzeliella* spp. and many other taxa.

Calcareous nannoplankton was investigated between 2612 and 2654 m depth. All samples from the Zupfing Formation (2612-2641 m) contain very well preserved, common autochthonous nannofossils with high percentages of *Cyclicargolithus floridanus*, *Coccolithus pelagicus*, and small reticulofenestrids (<3 μm). Rare but regularly occur: *Cyclicargolithus abisectus* (Müller) Wise, *Helicosphaera recta* Haq, *Pontosphaera desueta* (Müller) Perch-Nielsen, *Pontosphaera multipora* (Kamptner) Roth, *Reticulofenestra bisecta*, *R. clatrata* Müller, *R. lockeri*, *R. stavensis*, *Thoracosphaera saxea* Stradner, *Zygrhablithus bijugatus* (Deflandre) Deflandre. Very rare, but stratigraphically important, are: *Sphenolithus dissimilis* Bukry & Percival, and *Sphenolithus conicus* Bukry. *Reticulofenestra ornata* was observed in the sample at 2641 m depth. The Eggerding Formation (2642-2654 m) is barren in calcareous nannoplankton with the exception of the sample at 2648 m depth, which contains the same assemblage as the lower part of the Zupfing Formation.

5.1.5 Well Z

The complete lower Oligocene succession was investigated in well Z using cuttings samples. Well logs and the analytical data (Fig. 8) show a subdivision of the Schöneck Formation into a marly lower part with moderate TOC contents ("units a, b" according to Schulz et al., 2002) and a shaly upper part with very high TOC contents ("unit c"). The Dynow Formation is characterized by high carbonate and relatively low TOC contents.

The Eggerding Formation in well Z is characterized by carbonate contents around 10 % and TOC contents around 1.6 % (Fig. 8). Only the lowermost part of the Eggerding Formation exhibits slightly higher TOC contents (2.2 %). HI values in the Eggerding Formation range from 140 to 390 mg HC/g TOC ("true" HI: 520 mg HC/g TOC). The Transition Zone is 8 m thick and is characterized by both, high carbonate (30 %) and TOC contents (1.5 %). The average carbonate and TOC contents in the Zupfing Formation are 25 % and 1.1 %, respectively. HI in the organic-lean part of the Zupfing Formation ranges from 125 to 200 mg HC/g TOC ("true" HI: 275 mg HC/g TOC). The average Tmax is 428°C (Tab. 1).
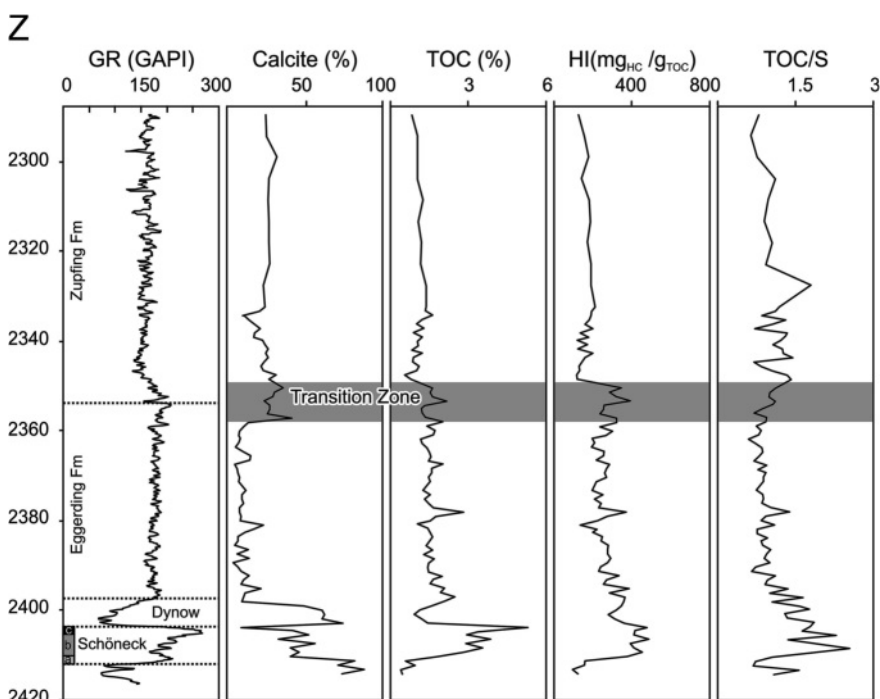

Figure 8: Gamma Ray (GR), calcite contents and source rock parameters of the Eggerding Formation in well "Z". All data were determined using cuttings samples.

Both, the Eggerding Formation and the Zupfing Formation are characterized by low TOC/S ratios. These are generally <1.0 in the Eggerding Formation and around 1.0 in the Zupfing Formation.

5.2 Carbon and Oxygen Isotopic Composition of Calcite

$\delta^{13}C$ and $\delta^{18}O$ values of calcite in the Lower Oligocene succession in wells Osch and P are shown in Fig. 9.

Dynow Formation: $\delta^{13}C$ and $\delta^{18}O$ values of calcite in carbonate-rich rocks of the Dynow Formation range from -1.1 to +0.7 ‰ and from -5.2 to -2.9 ‰, respectively. The low $\delta^{13}C$ and $\delta^{18}O$ values support the establishment of brackish conditions (Anderson and Arthur, 1983; Röhl et al., 2001). With the exception of the two lowermost samples, there is a good correlation between $\delta^{13}C$ and $\delta^{18}O$ (correlation coefficient $r^2 = 0.69$) arguing against a severe diagenetic alteration of the isotopic composition of these calcites and for a long residence time of the water body (closed system according to Talbot, 1990).

Eggerding Formation: The lower part of the Eggerding Formation is characterized by variable, but relatively high $\delta^{13}C$ (-0.5 to +1.8) and consistently low $\delta^{18}O$ (-5.0 to -4.4) values of calcite. Isotopically light $\delta^{18}O$ values indicate that low-salinity conditions persisted after deposition of the Dynow Formation. However, the lack of a positive correlation between $\delta^{13}C$ and $\delta^{18}O$ values suggests a transition to hydrodynamically open conditions (Talbot, 1990). Less negative $\delta^{18}O$ values of calcite in the uppermost sample in well Osch ($\delta^{13}C$: +2.0; $\delta^{18}O$: -3.3) transfer to values typical for the upper part of the Eggerding Formation. In this part $\delta^{13}C$ values are positive (+0.4 to +2.0) and $\delta^{18}O$ values range from -2.7 to -3.9. The results are in the range normally obtained from marine limestones (Anderson and Arthur, 1983).

Zupfing Formation: A major shift in $\delta^{13}C$ from calcite occurs at the base of Zupfing Formation, where $\delta^{13}C$ drops from about +1.5 to negative values (-2.5 to -0.1). This shift is accompanied by a change towards significantly higher calcite contents arguing for a dilution of the isotopic signal of marine cement by carbonate shells (coccolithophorides, foraminifera). In contrast to $\delta^{13}C$, there is no major shift in $\delta^{18}O$ values (-2.9 to -4.0).

5.3 Organic Geochemistry

In this section biomarker data from wells Osch (lower part of the Eggerding Fm.) and P (upper part of the Eggerding Fm., Zupfing Fm.) are compared.

n-Alkanes and isoprenoids – Because of higher maturity in well P, the Carbon-Preference-Index (CPI; calculated according to Bray and Evans, 1961) is generally higher in samples from well Osch (0.6-2.4) than in samples from well P (0.8-1.3). Within the lower part of the Eggerding Formation (Osch), two samples (72, 59) are characterized by relatively high proportions of long-chain C_{27}-C_{31} *n*-alkanes relative to the sum of *n*-alkanes and high CPI. This suggests a temporary high contribution of land plants to the organic matter in the lower Eggerding Formation of well Osch (Eglinton and Hamilton, 1967).

According to Didyk et al. (1978), pristane/phytane (Pr/Ph) ratios below 1.0 indicate anaerobic conditions during early diagenesis, and values between 1.0 and 3.0 were interpreted as reflecting dysaerobic environments. However, Pr/Ph ratios are known to be also affected by maturation (Tissot and Welte, 1984) and by differences in the precursors for acyclic isoprenoids (Volkman and Maxwell, 1986, Goossens et al., 1984, ten Haven et al., 1987). Because of the observed difference in maturity between wells Osch and P, only samples from the same well should be compared. Pr/Ph ratios within the lower part of the Eggerding Formation (Osch) vary significantly (2.32 to 0.61; Fig. 9). However, very low TOC/S ratios indicate that the Pr/Ph ratio is not a good redox indicator in the present case. Moreover, an excellent correlation between Pr/Ph ratios and the proportion of long-chain (C_{27}-C_{31}) *n*-alkanes (correlation coefficient $r^2 = 0.82$) suggests that the Pr/Ph ratio is mainly controlled by organic matter input. There is relatively little variation in the Pr/Ph ratios in samples from the upper part of Eggerding Formation and the lower part of the Zupfing Formation (0.88 -1.38; Fig. 9), which agree with an oxygen-depleted environment indicated by very low TOC/S ratios.
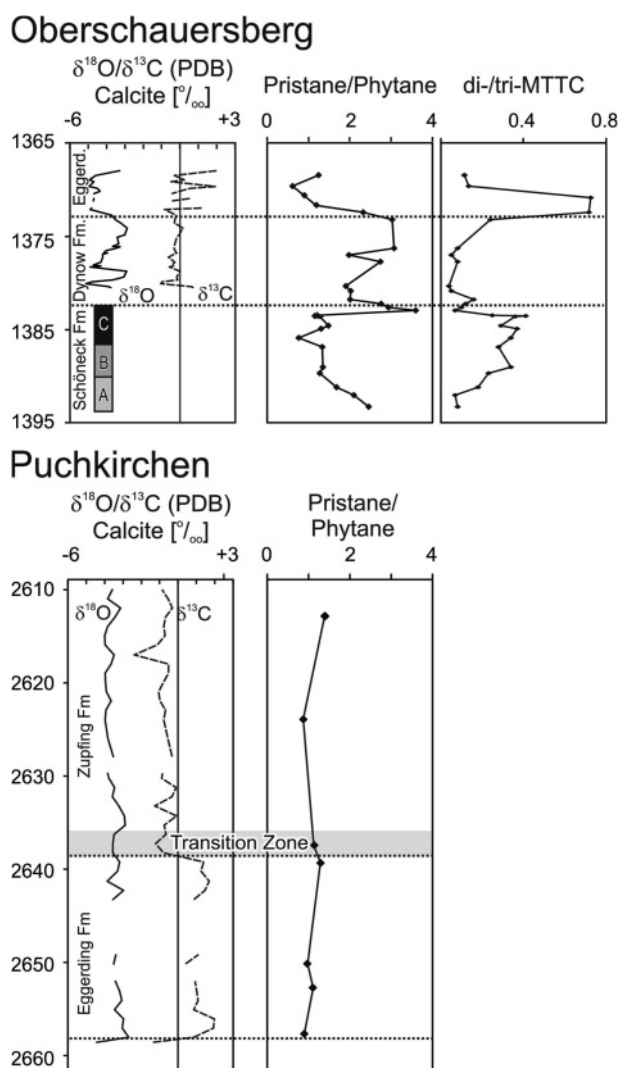

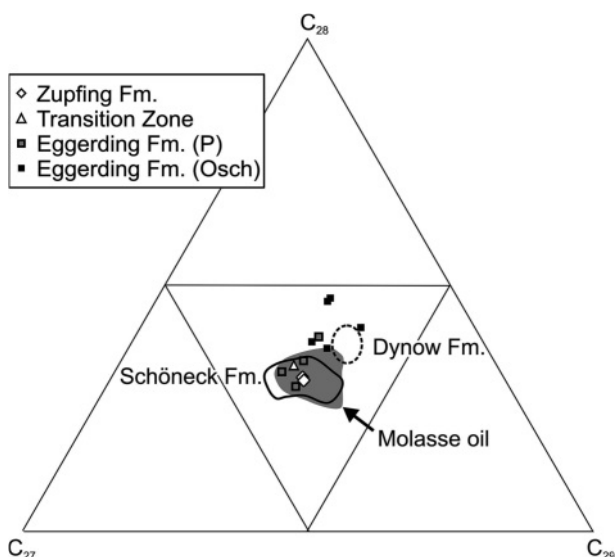**Figure 9:** Stable isotope composition of calcite and biomarker data.

FIGURE 10: Triangular plot of C_{27}, C_{28} and C_{29} steranes in samples from different Lower Oligocene formations. Data from Molasse oils are plotted for comparison (Gratzer et al., 2008).

Steroids and hopanoids – Beside regular steranes, diagenetically modified steranes (diasteranes) exist in the studied samples. There is little variation in the relative amount of C_{29} steranes (30-35 %), which are typically related with land plants (Volkman, 1986). Samples from the upper Eggerding Formation, the Transition Zone and the Zupfing Formation include a higher proportion of C_{27} steranes of algal origin (Fig. 10). In contrast, relatively high percentages of C_{28} steranes in the lower part of the Eggerding Formation might be related to the presence of layers with coccolithophorides (Grantham and Wakefield, 1988).

The most probable biological precursors of hopanes are bacteriohopanepolyols (Ourisson et al., 1979; Rohmer et al., 1992). These compounds have been identified in bacteria, as well as in some cryptogames (e.g. moss, ferns). Steranes/hopanes ratios, a measure of organic matter production by autothrophic eukaryotes (e.g. algae, land plants) versus bacterial activity, are positively correlated with TOC/S ratios and negatively correlated with the ratio of C_{27} and C_{28} steranes. Low sterane/hopane ratios are considered to indicate a lacustrine or a special, bacteria-influenced facies, whereas a high ratio is indicative of a marine organic facies (Mackenzie, 1984). This suggests a higher proportion of bacterially reworked organic matter and a strictly anoxic depositional environment in the upper Eggerding and the Zupfing formations (P). In contrast, a higher contribution of coccolithophorides (or dinoflagellates and diatoms), less microbial reworking and less strict anoxic conditions predominated in the lower part of the Eggering Formation (Osch).

The 20S/(20S+20R) isomer ratio of C_{29} steranes, the 22S/(22S+22R) isomer ratio of C_{31} hopanes, and the triaromatic steroids/(tri- + monoaromatic steroids) ratio are maturity indicators (Seifert and Moldowan, 1986). Higher ratios in samples from the deeper well P (Tab. 1) prove a slightly higher maturity (immature to marginal mature) compared to the immature

samples from the Osch well.

Chromans – Methylated 2-methyl-2-(trimethyltridecyl) chromans (MTTCs) occur in significant amounts only in the lower Eggerding Formation (Osch), where the 2,5,7,8-tetramethyl-2-(4',8',12'-trimethyltridecyl) chroman (tri-MTTC) predominates in all samples over the 2,5,8-trimethyl-2-(4',8',12'-trimethyltridecyl) chroman (di-MTTC; Fig. 9). Although the origin of methylated MTTCs is not yet understood, methylated MTTCs have been widely used for palaeosalinity reconstruction (Sinninghe Damsté et al., 1993; Barakat and Rullkötter, 1997). The di-/tri-MTTC ratio is proportional to the salinity.

Depth trends of the di-/tri-MTTC ratio in the Schöneck Formation, the Dynow Formation and the lower part of the Eggerding Formation are shown in Fig. 9. The di-/tri-MTTC ratio increases from unit a towards units b and c of the Schöneck Formation (Sachsenhofer and Schulz, 2006). In the upper part of unit c the ratio decreases abruptly and remains low within the Dynow Formation. Towards the Eggerding Formation the di-/tri-MTTC ratio rises again and reaches a maximum, before it drops to values similar to those in the Dynow Formation. Note that the Pr/Ph ratio is inversely proportional to the di-/tri-MTTC ratio, except for the lower part of the Eggerding Formation; here the Pr/Ph ratio does not follow the major fluctuations of the di-/tri-MTTC ratio.

5.4 Log Facies and Log Correlations

Major differences in log facies occur between the Eggerding Formation deposited in a marginal near-shore facies, the upper slope, the lower slope and the basin floor. The interfingering of pelitic rocks with sandstone characteristic for the Eggerding Formation deposited in near-shore environment causes serrated log patterns (e.g. Egdg; Fig. 4). An upward fining succession reflects decreasing terrestrial influence.

5.4.1 Upper Slope

The log facies of the Eggerding Formation deposited on the northern paleoslope of the Molasse Basin is typically characterized by high GR and low sonic velocities (high DT) (Figs. 4, 11). Within the Eggerding Formation the log pattern is relatively smooth, although some low-amplitude variations are visible. Apart from wells affected by faulting or erosion these log patterns can be traced over wide distances in a (coast-parallel) W-E direction (Fig. 11).

Whereas the thickness of the Eggerding Formation is typically between 40 and 45 m, Eggerding Formation with an outstanding thickness (~65 m) has been drilled in the well "F". A comparison with typical log patterns shows that the unusual thickness is due to material added in the upper part of the Eggerding Formation (Fig. 11). The log pattern of the additional material is unique, suggesting that the thickening is not a result of reverse faulting. We, therefore, propose that the exceptional thickness is due to re-deposited material mobilized in upslope positions. This implies that erosion was not restricted to the area west of the Lindach Fault.

In order to investigate the effect of erosion east of the Lind-

ach Fault, log patterns of two Voitsdorf wells (Va, V) are compared to that of well E, which is considered to contain a complete Eggerding Formation (Fig. 12). The correlation shows that up to 10 m of Eggerding Formation and a few meters of Zupfing Formation are missing in some Voitsdorf wells including the studied well V. This implies that erosion continued during the onset of deposition of the Zupfing Formation.

Whereas well F is the only example where the Eggerding Formation is exceptionally thick, its thickness is significantly reduced in many wells affected by erosion. The example of the Trattnach-Aistersheim area (Fig. 13) shows that erosion may cut into the Eocene limestones. Partly the originating paleo-topographic relief was filled with re-deposited(?) Eggerding Formation (Trat 4).

5.4.2 Lower Slope and Basin Floor

The Oberhofen 1 well drilled Eggerding Formation beneath the Alpine nappes in the authochthonous part of the Molasse Basin and in the allochthonous Molasse imbricates (Wagner et al., 1986). Whereas the authochthonous Eggerding Formation represents a lower slope environment, the Eggerding Formation in the Molasse imbricates represents an even more distal depositional realm (Wagner, 1998). The Eggerding Formation in both settings is characterized by strongly serrated log patterns (Fig. 14). Cuttings from the authochthonous part of the Oberhofen 1 well suggest that this is due to the presence of re-deposited Eocene (and lower Oligocene?) material (Sachsenhofer and Schulz, 2006).

5.5 Seismic Facies

The Lower Oligocene succession is characterized by parallel, continuous reflectors with varying amplitude. The top of the Eocene limestones and the top of the Schöneck Formation form prominent high-amplitude reflectors. In contrast, the tops of the Dynow and Eggerding formations, as well as the Zupfing Formation are characterized by parallel low-amplitude reflectors (Fig. 15).

In some areas the parallel reflectors are cut by erosional surfaces (Fig. 15). Erosional features are notably well visible in shallow portions of the basin, for example in the northern part of the Ried-Schwanenstadt Block. Here, an erosional channel, about 60 m deep and up to 20 km wide, occupies nearly the entire area of the tectonic block (Fig. 3). The basal unit of the
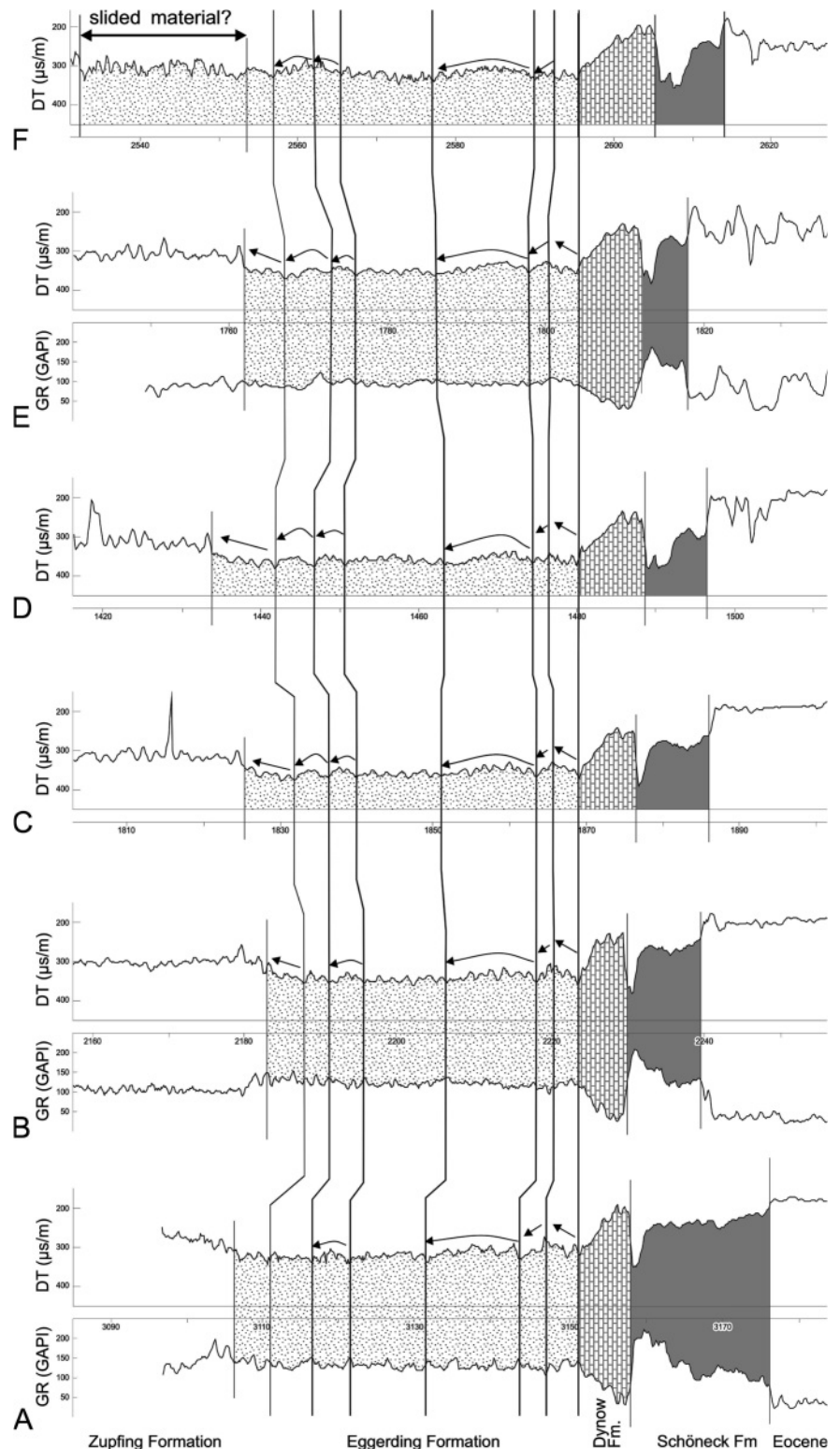

Figure 11: GR and DT logs from „key wells". Some log patterns within the Eggerding Formation are indicated by arrows. These patterns can be correlated over more than 100 km in a W-E direction.

Zupfing Formation onlaps onto the margins of the erosive channels.

The erosional surface is either smooth (e.g. Fig. 15b, d) or highly structured (Fig. 15a). Chaotic reflection patterns along the western part of Fig. 15a suggest the presence of several early Oligocene erosion events.

An isopach map of the interval between "base Eocene unconformity" and the erosional unconformity near "top Eggerding Formation" in the central part of the Ried-Schwanenstadt Block (Fig. 16) together with two N-S-trending seismic sections (Fig. 15c, d) and the Trattnach-Aistersheim logs (Fig. 13) provide further insights into the processes resulting in erosion of the Eggerding Formation.

The lower Oligocene succession is largely complete in the northeastern edge of the map, but totally eroded in the southern part. This latter is confirmed by wells, where erosion cut into the Eocene Lithothamnium Limestone. Consequently the thickness of the interval between "base Eocene" and "base Zupfing" (="top Eggerding") in these wells is only 25 to 31 m.

The thickness distribution in the northwestern part of the map presented in Fig. 16 suggests a significant reduction in thickness of the Lower Oligocene succession. Reflection configuration along the northern part of the section shown in Fig. 15c indicates the presence of a submarine slide with intense deformation of the preserved lower Oligocene succession. We, therefore, interpret the "greenish" body in the northwestern part as a mega-slide. Partly the slided material intruded into its frontal parts (Fig. 15c). This shows that the slide preserved considerable stiffness. Perhaps this is because of the presence of Dynow Formation. The headscarp of the mega-slide is not well resolved in Fig. 15c.

The head-scarp of another slide is visible in Fig. 15d and reveals a stair-like topography. We speculate that this is due to movements along well-defined slippage planes (e.g. above and/or below the Dynow Fm.). Within this context it is remarkable to observe that the complete Schöneck Formation is preserved in well Trat 11, whereas the Dynow Formation is removed (Fig. 13).

6. Discussion and Interpretation

6.1 Age Constraints

The co-occurrence of dinoflagellates taxa such as *Wetzeliella gochtii*, *Wetzeliella articulata*, *Rhombodinium draco*, *Chiropteridium galae*, *Chiropteridium lobospinosum*, *Enneadocysta pectiniformis* strongly suggests a Late Rupelian age for the Eggerding Formation (Wilpshaar et al., 1996; Torricelli and Biffi, 2001; Williams et al., 2004). *Distatodinium biffii* is found in samples from the Zupfing Formation (20, 30), whereas *Wetzeliella articulata* is missing. This implies a ?late Rupelian-early Chattian age of the Zupfing Formation (e.g. Van Simaeys et al., 2005).

Additional information is provided by calcareous nannoplankton. The studied interval overlies the Dynow Formation dated as lower/middle nannoplankton zone NP23 (middle Rupelian; Bubik, 1991; Schulz et al., 2004). NP23 is defined as the period between the last appearance of *Reticulofenestra umbilica* (Levin) Martini & Ritzkowski and the initial appearance of *Sphenolithus cipero-*
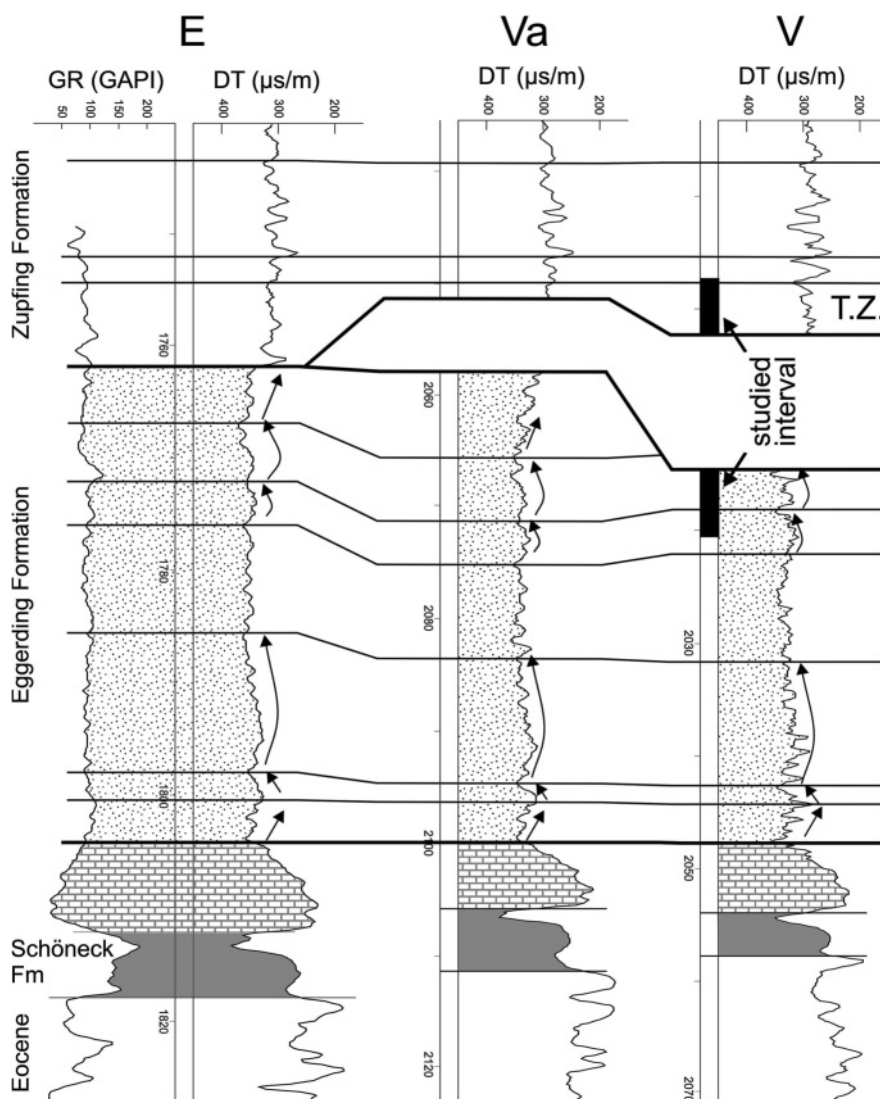

FIGURE 12: Wire-line logs of well E (Fig. 4) and two wells in the Voitsdorf field (Va, V). The base of the Eggerding Formation and a prominent peak in the DT log in the lower Zupfing Formation are used as datum. The correlation shows that a few meter of uppermost Eggerding and lowermost Zupfing formation are missing in the Voitsdorf wells. Seismic lines show that this is not due to (seismic-scale) faulting.
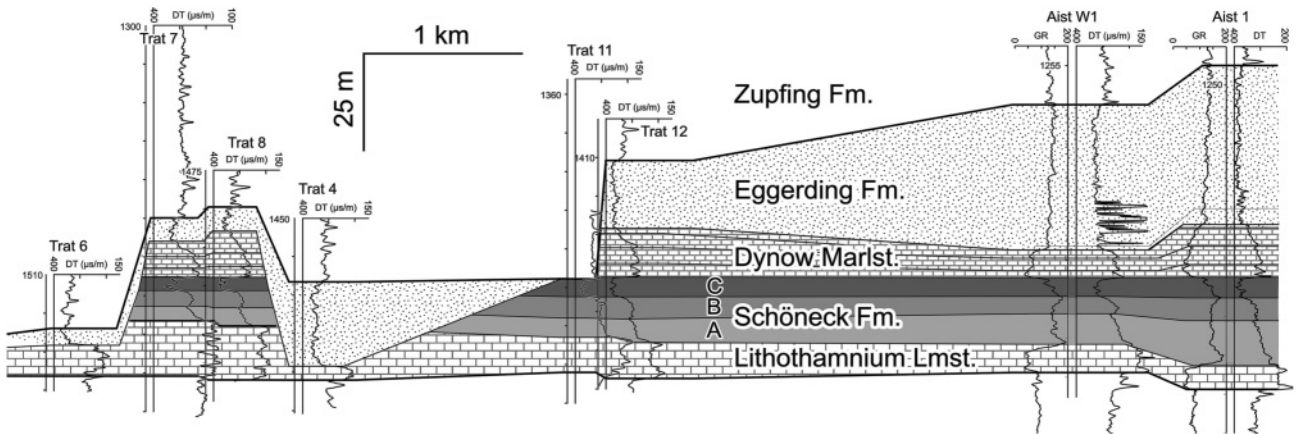
FIGURE 13: GR and DT logs of Trattnach and Aistersheim wells. See Fig. 167 for location of cross-section.

ensis Bramlette & Wilcoxon (Martini, 1971). The lack of *S. ciperoensis* in the investigated samples of the Eggerding Formation and the lower part of the Zupfing Formation supports NP23. However, in contrast to *R. umbilica*, *S. ciperoensis* appears only sporadically in sediments of the Central Paratethys and, therefore, is not a useful marker for NP24 in this bioprovince (see also Garecka, 2005).

Important to note, that the lower part of the Zupfing Formation (incl. the Transition Zone) in borehole P contains *Helicosphaera recta* which has its lowest occurrence at the NP 23/24 boundary (Müller, 1970). This and the absence of typical endemic taxa, which occur in NP23 confirm an attribution of this formation into NP24 (upper Rupelian/lower Chattian).

Apart from zonal markers, bio-events caused by paleogeographical and paleoecological changes are important for the stratigraphic subdivision of Oligocene sediments in the Central Paratethys. The predominantly non-calcareous Šitborice Member of the Menilitic Formation in the western Carpathian Foreland Basin (NE Vienna) overlies the Dynow Marlstone and is about 40 m thick (Picha and Stranik, 2005). It is considered a time-equivalent to the Eggerding Formation and the lowermost Zupfing Formation (Fuchs et al., 2001). Among five low-diversity assemblages in the Šitborice Member, Bubik (1991) recognized an assemblage
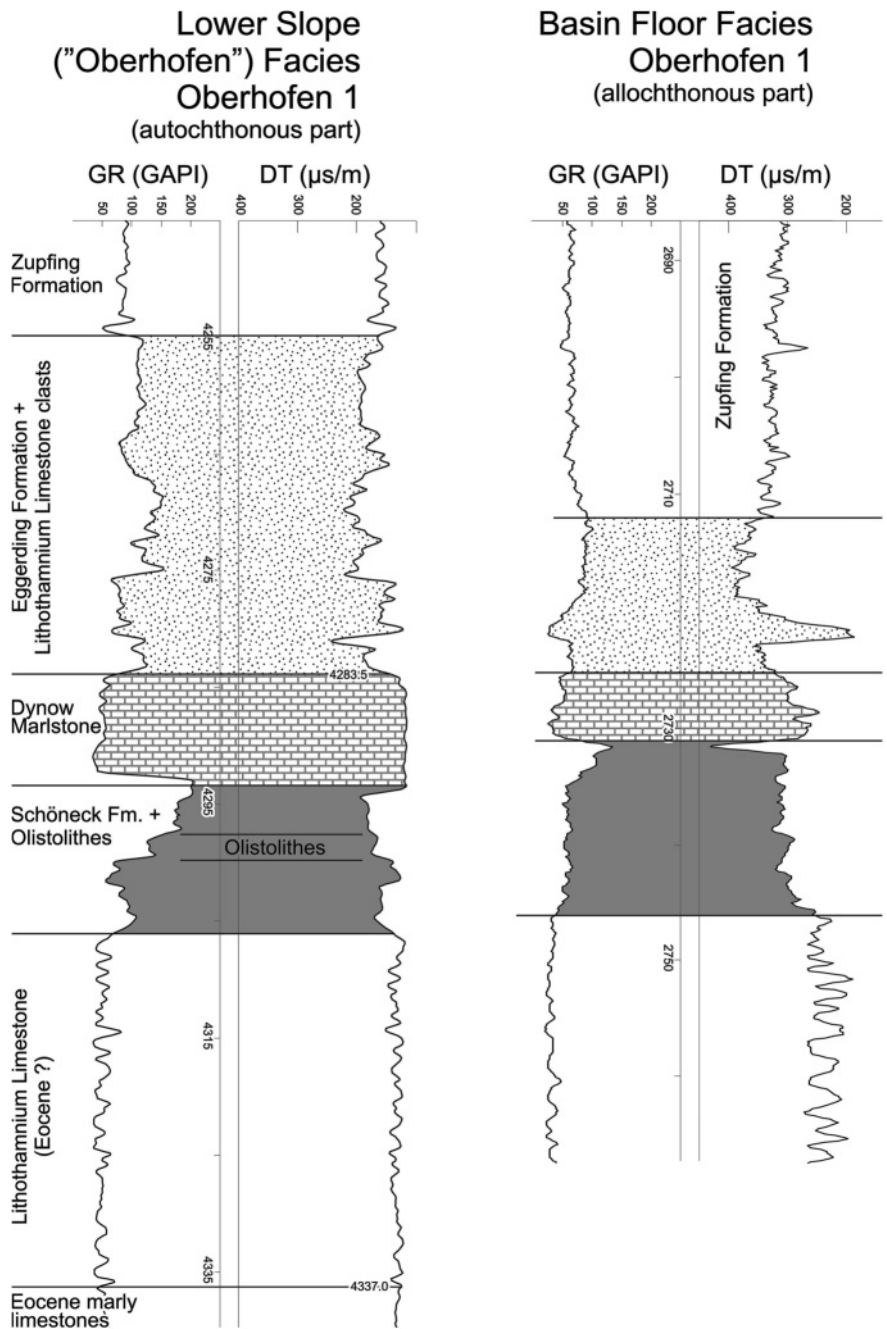

FIGURE 14: GR and DT logs of well Oberhofen 1.

with a high dominance of *Cyclicargolithus floridanus*. This horizon is placed into upper NP23 to lower NP24.

Melinte (2005) investigated Oligocene sediments in the Romanian Carpathians and detected identical nannoplankton assemblages as in the Eggerding Formation. In this basin blooms of *C. floridanus*, *R. bisecta*, *R. ornata* and *S. moriformis* occurred during (the upper NP23 and) NP24 and can be correlated with similar events in the Molasse Basin. High percentages of these forms indicate a co-eval bio-event caused by warmer climate mode during this part of the Oligocene (Melinte, 2005).

6.2 Depositional Environment

6.2.1 Near-shore environment

Eggerding Formation deposited in near-shore environments (e.g. borehole Egdg) is characterized by frequent sand layers. Clasts of reworked Dynow Formation in well Egdg indicate erosion after deposition of the Dynow Formation. The latter has a very wide northward extension and is overlain by sandy sediments in several wells located near the northern basin margin. This suggests that the maximum flooding event occurred during deposition of the Dynow Formation. The general upward decrease in thickness and frequency of sandstone layers within the Eggerding Formation in well Egdg suggests another transgression during deposition of the Eggerding Formation. Nevertheless it remains unclear whether erosion at the site of well Egdg is due to a lowering of the sea level or due to submarine erosion at the northern flank of the Molasse Basin (see section 6.3).

Oxygen-depleted conditions are indicated by very low TOC/S ratios (Fig. 6). This finding is supported by palynofacies analysis. AOM and variable amounts of phytoclasts are the dominant palynological elements suggesting a proximal to distal suboxic-anoxic shelf setting (Fig. 17). In addition, the dominance of the green algae Pediastrum indicates an estuarine/brackish environment (Brown and Downie, 1984).
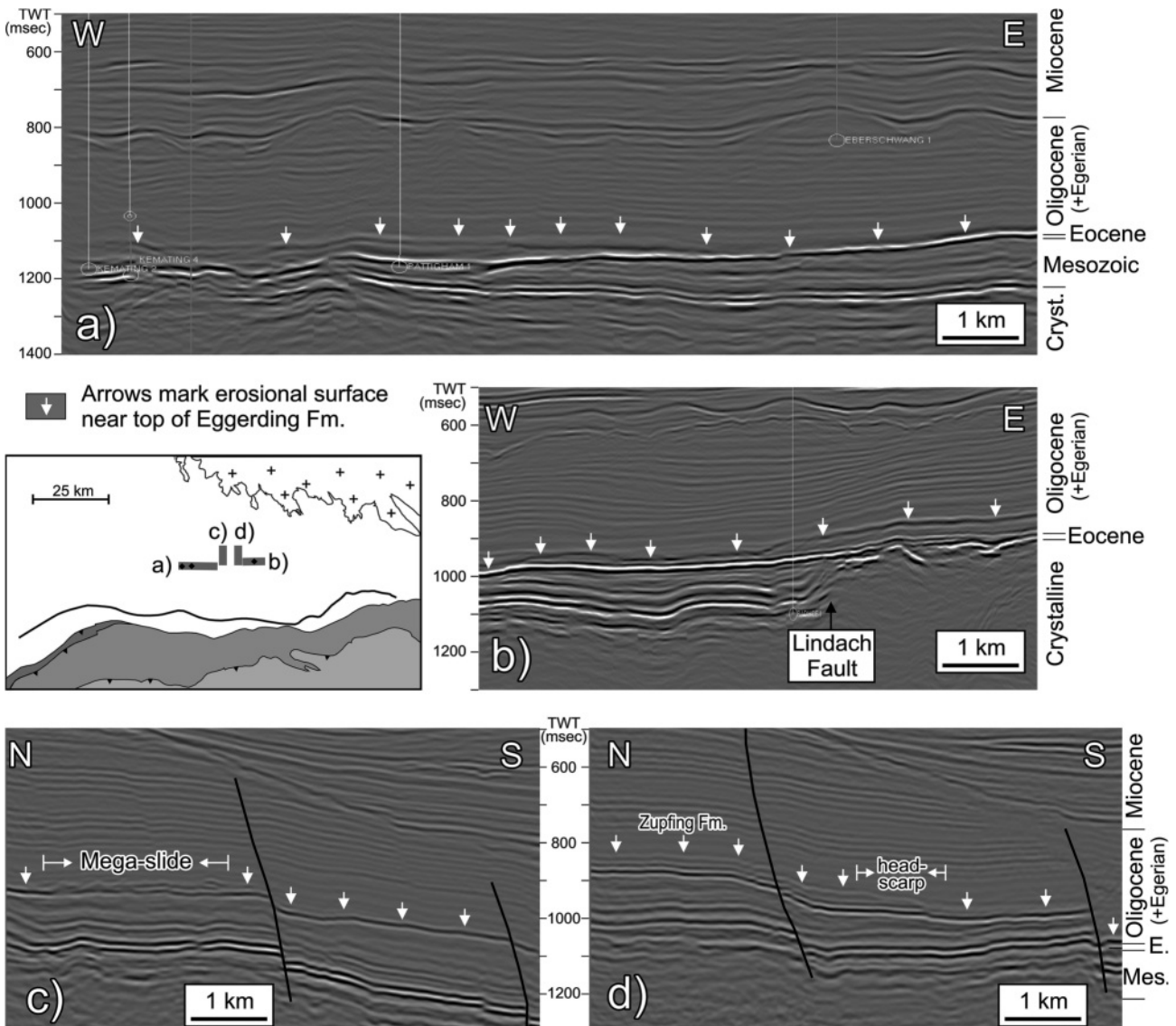

FIGURE 15: W-E- and N-S-trending seismic sections showing erosional features near the top of the Eggerding Formation. (a, b are taken from Sachsenhofer and Schulz, 2006).

6.2.2 Upper Slope

Similar to the Schöneck and Dynow formations, logs of the Eggerding Formation in upper slope settings indicate high lateral continuity. This observation suggests uniform sedimentation in the deep marine Molasse Basin during early Oligocene time. Mass movements across the southward inclined slope during deposition of the Eggerding Formation are witnessed by submarine slides (Figs. 15, 16) and slumps visible in borehole (FMI) logs.

With the exception of wells affected by erosion, the transition between the Dynow and Eggerding formations in upper slope settings is gradual. However, it is characterized by a significant decrease in carbonate production.

Lime- and marlstones of the Dynow Formation have been formed by cyclic blooms of coccolithophorids; such thin white bands composed of calcareous nannoplankton within the Eggerding Formation are restricted to its lowermost part.

Schulz et al. (2004) speculate that increased photic zone anoxia and an increase in salinity worsened the ecological environment for calcareous nannoplankton and led to the deposition of marls of the Eggerding Formation during the late NP23.

The observed increase in the di/tri-MTTC ratio near the base of the Eggerding Formation in well Osch points to increasing salinities and is consistent with this hypothesis. Low TOC/S ratios (~1.6), low Pr/Ph ratios and the lack of bioturbation indicate that oxygen-depleted conditions continued during deposition of the lower part of the Eggerding Formation, although aryl-isoprenoids characteristic for photic zone anoxia were not detected. Anoxic conditions in a distal environment are also suggested by the palynofacies of Osch samples (Fig. 17a,b).

A few meters above the base of the Eggerding Formation di-/tri-MTTC ratios are low again indicating strong variations in salinity during deposition of the lower part of the Eggerding Formation.

Periods with low salinity are indicated also by samples rich in *Braarudosphaera bigelowii*. This form is especially frequent in near shore environments. Nagymarosy (1991) described the Braarudosphaera-bloom from Oligocene sediments and explained it with the partial separation of the Paratethys, whereas Bukry

(1974) used the high percentage of *B. bigelowii* in Holocene sediments from the Black Sea as an indication of low marine salinity. Thus, the enrichment of this cold, nutrient-rich water-preferring species in sediments suggests short periods of fresh water input and reduced salinity during deposition of the lower part of the Eggerding Formation.

Sandstone layers are abundant in the lower part of the Eggerding Formation in borehole Osch. Moreover, coarsening upward trends near the base of the Eggerding Formation (Fig. 11) may indicate increasing detrital input caused by strong surface water run-off.

In comparison to the lower part of the Eggerding Formation, the environment during deposition of its upper part (studied in boreholes V and P) was relatively stable. Palynofacies suggests that (suboxic to) anoxic conditions persisted (Fig. 17b).

Marine palynomorphs, dinoflagellate cysts, are persistent with variable abundance in all samples. The encountered dinoflagellate cyst assemblage reflects a neritic environmen
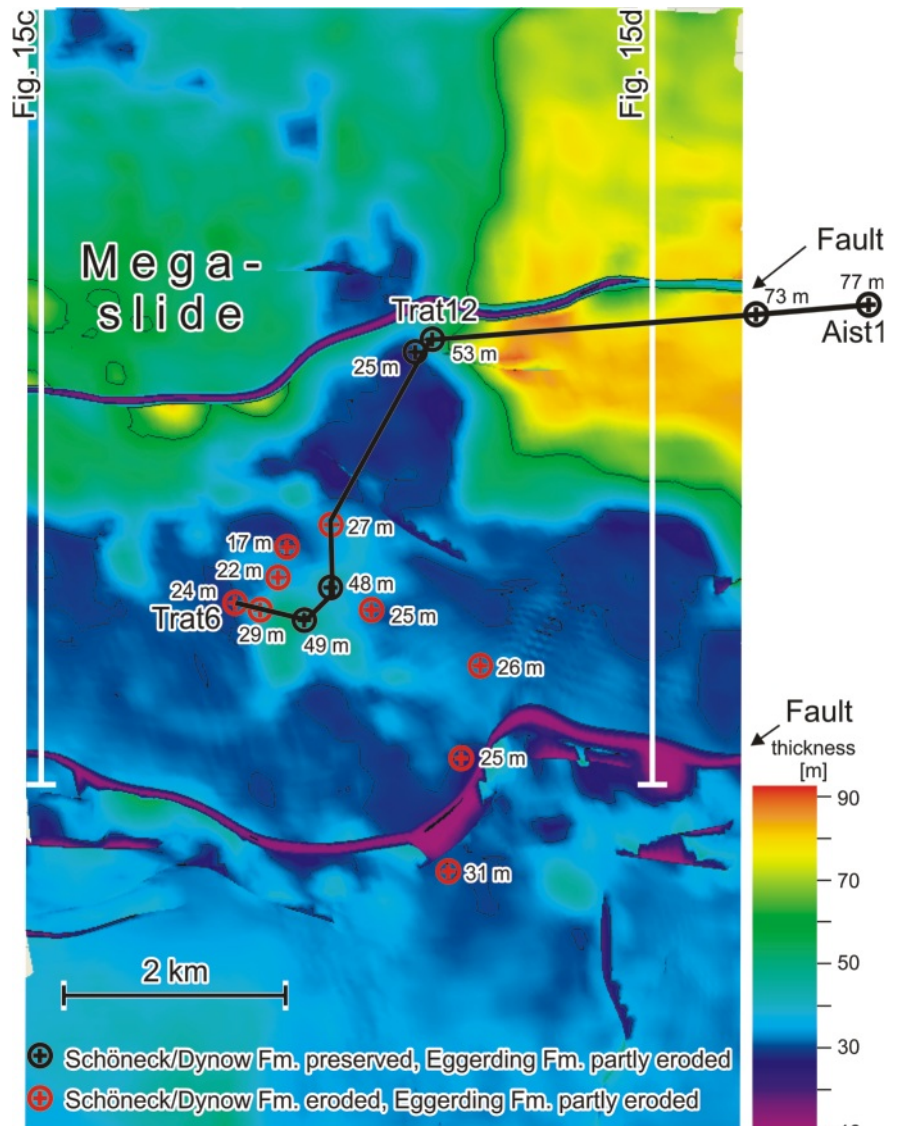

Figure 16: Isopach map of interval between base Eocene unconformity and top Eggerding Formation.

during the deposition of the Eggerding Formation as well as the lowermost part of Zupfing Formation. This conclusion is based on the presence/dominance of *Homotryblium* spp., *Wetzeliella* spp., *Deflandrea* spp., and *Glaphyrocysta* spp. (Islam, 1984; Köthe, 1990; Brinkhuis, 1994; Dale, 1996; Head et al., 2005; Plate 1). On the other hand, the abundance of the heterotrophic taxa as *Lejeunecysta* and *Selenopemphix* as well as *Deflandrea* in samples of the upper Eggerding Formation (well P) clearly reflects nutrient rich surface water during deposition (Brinkhuis et al., 1992, Dale, 1996).

Blooms of *Cyclicargolithus floridanus* occur in the lower Zupfing Formation, both in the organic-rich Transition Zone (P18, 2639 m depth) and the overlying organic-poor Zupfing Formation (P22: 2635 m; P28: 2626 m).

6.3 Slope Instability and Submarine Erosion

A major erosional event occurred around the transition of the Eggerding and Zupfing formations (see also Sachsenhofer and

Figure 17: a) AOM - Palynomorph - Phytoclast ternary diagram (after Tyson, 1995) of the relative numerical particle frequenty (% of the total sum of organic matter). b) AOM - Phytoclasts+Sporomorphs - Foraminiferal test lining + Dinoflagellates + Acritarchs + other marine algae diagram (modified from Tyson, 1995) of the relative numerical particle frequency (% of the total sum of organic matter).

Schulz, 2006). The lower Oligocene formations were deposited in several hundred metres of water depth (Wagner, 1998). Therefore even a major sea level fall comparable to that between the early and late Oligocene could not establish subaerial conditions. Consequently, erosion is considered a submarine processes (Sachsenhofer and Schulz, 2006).

In some wells submarine slides from the northern slope of the Molasse Basin removed rocks up to 70 m thick (Eggerding Fm., Dynow Fm., Schöneck Fm.) and cut into the Eocene limestones (see wells with open symbols in Fig. 3). Erosion was especially prominent west of the Lindach Fault. 3D seismic data show the presence of major E-W orientated slide scarps and minor N-S orientated slide scarps along the sidewalls of the slides. Log patterns of wells Obhf 1 and Grünau 1 suggest that the slided material was deposited near the base of the northern slope of the Molasse Basin. However, locally slided material was also deposited on the upper slope. This is shown i.a. by the presence of a large sediment body characterized by undulating reflectors north of the Trattnach field, which covers several square kilometres. Fig. 15d suggests that failure planes existed both above and below the mechanically stiff Dynow Formation. Blocks of Schöneck Formation and Dynow Formation drilled in boreholes Trat 7 and Trat 8 were interpreted as erosional remnants (Sachsenhofer and Schulz, 2006). However, in the light of the new seismic data, they might constitute rafted blocks.

Minor erosion occurred also in the area east of the Lindach Fault (e.g. Voitsdorf Field). Moreover, redeposited Eggerding Formation overlying authochthonous Eggerding Formation in well F suggests sliding in upslope position. Slope instability is also indicated by slumps detected by FMI logs in a well north of well F.

The age of the event is not yet completely clear. Because a Chattian age of the Zupfing Formation (former "Rupelian Marl") is likely, the erosion event might be related to the major sea level drop at the Rupelian/Chattian boundary. However, an intra-Rupelian event (related to the "Intra-Rupelian Unconformity" of Sissingh, 1997) cannot be excluded. Most probably the submarine slides were triggered by earth quakes related to the reactivation of Mesozoic faults such as the Lindach Fault.

Similar erosional events are indicated by the presence of slump bodies and debris flows in the Šitborice Member of the Menilitic Formation in the western Carpathians during NP23 ("Šitborice Event"; Krhovský and Djurasinovic, 1993). Correlations of such events highlight that slope instability may have occurred basin-wide and tectonically triggered rather than being a local phenomenon (Sachsenhofer and Schulz, 2006).

6.4 Hydrocarbon Potential and Correlation between Rock Extracts and Accumulated Oils

Using the terminology of Peters (1986), TOC contents between 1.9 and 6.0 % and HI values up to 600 mg HC/g TOC (Fig. 18) classify the lowermost part of the Eggerding Formation in the Osch well as a "very good" source rock for oil. The
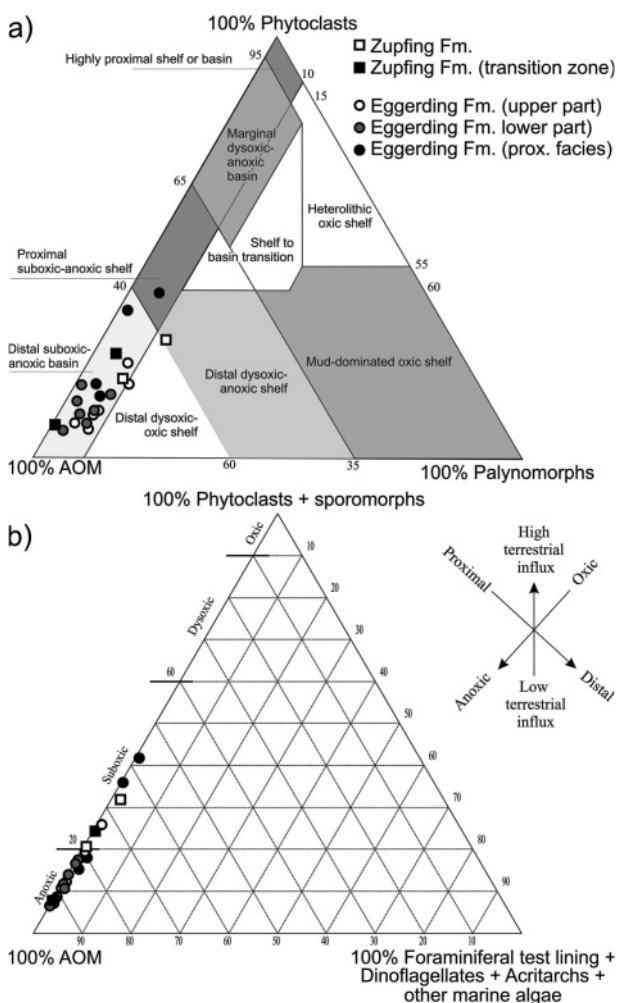
upper part of the Eggerding Formation and the Transition Zone (TOC: ~1.5 %; "true" HI 500-600 mg HC/g TOC) is oil-prone and a "good" source rock.

Demaison and Huizinga (1994) introduced a Source Potential Index (SPI) to quantify the hydrocarbon potential of source rocks (SPI = h* (S1+S2)*ρ/1000), where h is thickness, S1+S2 the genetic potential determined by RockEval pyrolysis and ρ rock density. Table 2 shows that the SPI of the Eggerding Formation is higher than that of the Schöneck Formation. This is mainly a result of its higher thickness.

Sterane distribution and Pr/n-C_{17} versus Ph/n-C_{18} plots have proven valuable in oil-source rock correlations (Connan and Cassou, 1980; Peters et al., 2005).

The triangular sterane plot (Fig. 10) shows an excellent fit between extract from the Schöneck Formation, the upper part of the Eggerding Formation, and the Transition Zone with Molasse oils. In contrast, the fit with extracts from the Dynow Formation and the lower Eggerding Formation is poor, suggesting that these rocks contributed only to a minor extent to the Molasse oil.

In the Pr/n-C_{17} versus Ph/n-C_{18} diagram the upper part of the Eggerding Formation and the Transition Zone show a better fit with Molasse oils than the lower part of the Eggerding Formation and the Schöneck Formation (Fig. 19). The Dynow Formation can be excluded as a major contributor to the Molasse oil based on this diagram.

More detailed biomarker and isotope investigations are needed to ascertain the oil-source rock correlation. However based on present knowledge both the Schöneck and the Eggerding Formation contributed to the Molasse oil. A minor contribution of the lower Eggerding Formation might have caused a distortion of the Molasse oil in Fig. 10 towards higher C_{28} sterane values.

7. Conclusion

The Eggerding Formation, about 45 m thick, forms parts of the Oligocene deep water succession in the Molasse Basin, which comprises from bottom to top the Schöneck, Dynow, Eggerding and Zupfing formations. The most important results of the study include:

● The Dynow Formation and the lower part of the Eggerding

Formation		S1+S2 [mg HC/g rock]	Thickness [m]	density	SPI [tHC/m²]
	„Transition Zone"	5.2	4	2	0.04
Eggerding Fm.	Upper part	5.6	37	1.9	0.39
	Lower part	15.9	5	1.9	0.15
				Σ Eggerding Fm.	0.58
Dynow Fm.		10.0	8	2	0.16
Schöneck Fm.		16.7	10	2.1	0.35
				Σ Lower Oligocene	1.09

TABLE 2: Genetic potential (S1+S2), average thickness, density, and Source Potential Index (SPI) of different lower Oligocene formations.
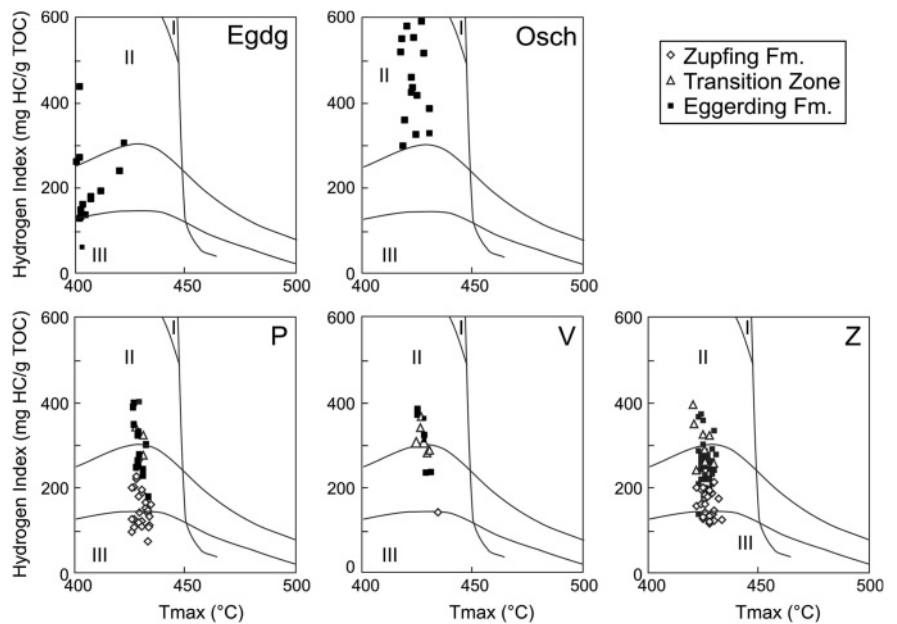

FIGURE 18: Plot of Hydrogen Index versus Tmax for Eggerding and Zupfing formations in different wells.
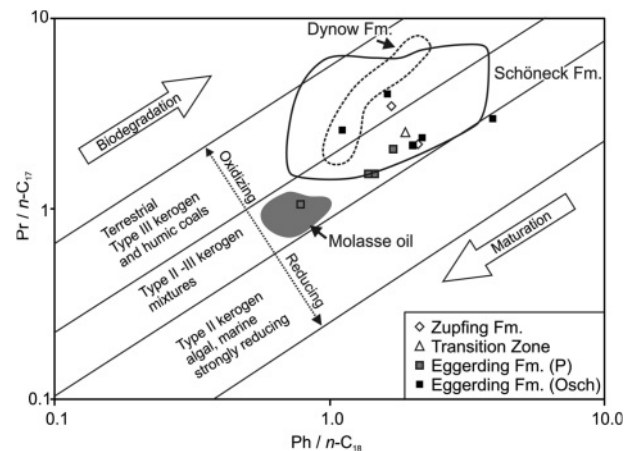

FIGURE 19: Pr/n-C_{17} versus Ph/n-C_{18} diagram.

Formation have been deposited during nannoplankton zone NP 23 (Rupelian), whereas the base of the Zupfing Formation was deposited during NP 24 (Rupelian to Chattian). A

?late Rupelian-early Chattian age of the lower part of the Zupfing Formation is suggested based on dinoflagellate cysts.

- The transition between the Dynow and Eggerding formations is characterized by a gradual decrease in carbonate contents. In contrast, the boundary between the Eggerding Formation and the overlying Zupfing Formation is sharp and characterized by an increase in carbonate contents.

- The Eggerding Formation has been deposited in an oxygen-deficient environment on the northern slope of the Molasse Basin. Its lower part consists of dark grey laminated shaly marlstone with white bands rich in coccolithophorides. TOC contents are about 5 %. The upper part of the Eggerding Formation consists of a homogenous sequence of marly shale and includes about 1.6 % TOC. Whereas marine palynomorphs are present in all samples from the Eggerding Formation, calcareous nannoplankton is restricted to its lower part. Salinity variations are recorded in rocks of the lower part of the Eggerding Formation. The environment during deposition of its upper part was more stable. Borehole logs show the high lateral continuity of the Eggerding Formation deposited on the upper slope. Thick sandy layers occur in near-shore environments.

- Slope instabilities are indicated by slumps within the Eggerding Formation and extensive submarine slides. Sliding reached a maximum at the transition from the Eggerding to the Zupfing Formation, when locally a succession up to 70 m thick was removed from the northern slope. In the area west of the Lindach Fault the base of the slides cuts into the Eocene limestones. The slided material was redeposited either on the northern slope (e.g. Trattnach area and well F) or at the base of the slope (e.g. Obhf 1).

- The Eggerding Formation is overlain by the Zupfing Formation, consisting of clay marl up to 450 m thick. Oxygen-depleted conditions continued during deposition of the Zupfing Formation, but only the lowermost few meters of the Zupfing Formation (Transition Zone) are organic matter rich (1.5 % TOC).

- Using the terminology of Peters (1986), the lower part of the Eggerding Formation (TOC 1.9-6.0 %; HI up to 600 mg HC/g TOC) is a "very good" source rock for oil. The upper part of the Eggerding Formation and the Transition Zone (TOC: ~1.5 %; "true" HI 500-600 mg HC/g TOC) is oil-prone and a "good" source rock.
Biomarker data suggest that the upper part of the Eggerding Formation and the Transition Zone contributed significantly to the Molasse oils, besides the Schöneck Formation which is probably the main source for these oils. In contrast, the contribution of the Dynow Formation and the lower Eggerding Formation was minor.

Acknowledgments

References

Anderson, T.F. and Arthur, M.A., 1983. Stable isotopes of oxygen and carbon and their application to sedimentologic and palaeoenvironmental problems. In: M.A. Arthur, T.F. Anderson, I.R. Kaplan, J. Veizer and L.S. Land (eds.), Stable isotopes in sedimentary geology. Society of Economic Palaeontologists and Mineralogists, Tulsa, Short Course No. 10, 151 pp.

Bachmann, G.H., Müller, M. and Weggen, K., 1987. Evolution of the Molasse Basin (Germany, Switzerland). Tectonophysics, 137, 77-92.

Barakat, A.O. and Rullkötter, J., 1997. A comparative study of molecular paleosalinity indicators: chromans, tocopherols and C20 isoprenoid thiophenes in Miocene lake sediments (Nördlinger Ries, Southern Germany). Aquatic Geochemistry, 3, 169-190.

Batten, D.J., 1996. Palynofacies and palaeoenvironmental interpretation. In: J. Jansonius and D.C. McGregor (eds.) Palynology: Principals and Applications vol. 3, American Association of Stratigraphic Palynologists Foundation, Dallas, Texas, pp. 1011-1064.

Batten, D.J. and Stead D.T., 2005. Palynofacies analysis and its stratigraphic application. In: E.A.M. Koutsoukos (ed.) Applied Stratigraphy, Springer, Dordrecht, pp. 203-226.

Berner, R.A., 1984. Sedimentary pyrite formation: An update. Geochimica et Cosmochimica Acta, 48, 605-615.

Bray, E.E. and Evans, E.D., 1961. Distribution of n-paraffins as a clue to recognition of source beds. Geochimica Cosmochimica Acta, 22, 2-15.

Brinkhuis, H., 1994. Late Eocene to Early Oligocene dinoflagellate cysts from the Priabonian type-area (northeast Italy): biostratigraphy and paleoenvironmental interpretation. Palaeogeography, Palaeoclimatology, Palaeoecology, 107, 121-163.

Brinkhuis, H., Powell, A.J. and Zevenboom, D., 1992. High-resolution dinoflagellate cyst stratigraphy of the Oligocene/Miocene transition interval in Northwest and central Italy. In: M.J. Head and J.H. Wrenn (eds.), Neogene and Quaternary Dinoflagellate Cysts and Acritarchs, Publishers Press, Salt Lake City, pp. 219-258.

Brix, F. and Schultz, O. (eds.), 1993. Erdöl und Erdgas in Österreich. Naturhistorisches Museum Wien, Horn, 688 pp.

Brown, S. and Downie, C., 1984. Dinoflagellate Cyst Biostratigraphy of Late Paleocene and Early Eocene Sediments from holes 552, 553 A, and 555, Leg 81, Deep Sea Drilling Project (Rochael Plateau). Initial Report D. S. D. P., 81, Washington, pp. 556-579.

Bubik, M., 1991. Low diversity calcareous nannoplankton assemblages from the Oligocene Sitborice Member of the Menilitic Formation (West Carpathians, Czechoslovakia) from Bystrice nad Olsi. In: B. Hamrsmid and J.Young (eds.), Proceedings of the 4th INA Conference, Prague 1991, Nannoplankton Research, Vol. II: Tertiary Biostratigraphy and Paleoecology; Quaternary coccoliths, Prague, pp. 223-246.

Bukry, D., 1974. Coccoliths as paleosalinity indicators - evidence from Black Sea. In: E.T. Degens and D.A. Ross (eds.), The Black Sea - Geology, Chemistry and Biology. American Association of Petroleum Geologists Memoir, 20, Tulsa, pp. 353-363.

Connan, J. and Cassou, A.M., 1980. Properties of gases and petroleum lipids derived from terrestrial kerogen at various maturation levels. Geochimica et Cosmochimica Acta, 44, 1-23.

Covault, J.A., Hubbard, S.M., Graham, S.A., Hinsch, R. and Linzer, H.-G., 2009. Turbidite-reservoir architecture in complex foredeep-margin and wedge-top depocenters, Tertiary Molasse foreland basin system, Austria.

Marine and Petroleum Geology, 26, 379-396.

Dale, B., 1996. Dinoflagellate cyst ecology: modeling and geological applications. In: J. Jansonius and D.C. McGregor (eds.), Palynology: Principals and Applications vol. 3, American Association of Stratigraphic Palynologists Foundation, Dallas, Texas, pp. 1249-1275.

de Ruig, M.J. and Hubbard, S.M., 2006. Seismic facies and reservoir characteristics of a deep-marine channel belt in the Molasse foreland basin, Puchkirchen Formation, Austria. American Association of Petroleum Geologists Bulletin, 90, 735-752.

Demaison, G. and Huizinga, B.J., 1994. Genetic classification of petroleum systems using three factors: charge, migration and entrapment. In: L.B. Magoon and W.G. Dow (eds.), The petroleum system, from source to trap. American Association of Petroleum Geologists Memoir, 60, 73-89.

Didyk, B.M., Simoneit, B.R.T., Brassell, S.C. and Eglinton, G., 1978. Organic geochemical indicators of paleoenvironmental conditions of sedimentation. Nature, 272, 216-222.

Dohmann, L., 1991. Die unteroligozänen Fischschiefer im Molassebecken. PhD Thesis, Ludwig-Maximilian-Universität, Munich.

Eglinton, G. and Hamilton, R.J., 1967. Leaf epicuticular waxes. Science, 156, 1322-1335.

Espitalié, J., Laporte, J.L., Madec, M., Marquis, F., Leplat, P., Paulet, J. and Boutefeu, A., 1977. Méthode rapide de caractérisation des roches meres, de leur potentiel pétrolier et de leur degré devolution. Revue Institut francais du Petrole, 32, 23-42.

Fensome, R.A., MacRae, R.A. and Williams, G.L., 2008. DINO-FLAJ2, Version 1. American Association of Stratigraphic Palynologists, Data Series no. 1. (http://dinoflaj.smu.ca/wiki/Main_Page).

Fuchs, R., Hamrsmid, B., Kuffner, T., Peschel, R., Rögl, F., Sauer, R. and Schreiber, O.S., 2001. Mid-Oligocene Thomasl Formation (Waschberg Unit, Lower Austria) – micropaleontology and stratigraphic correlation. In: W.E. Piller and M.W. Rasser (eds.), Paleogene of the Eastern Alps. Österreichische Akademie der Wissenschaften. Schriftenreihe der Erdwissenschaftlichen Kommissionen, 14, 255-290.

Garecka, M., 2005. Calcareous nannoplankton from the Podhale Flysch (Oligocene-Miocene, Inner Carpathians, Poland). Studia Geologica Polonica, 124, 353-369.

Genser, J., Cloetingh, S.A.P.L. and Neubauer, F., 2007. Late orogenic rebound and oblique Alpine convergence: New constraints from subsidence analysis of the Austrian Molasse basin. Global and Planetary Change, 58, 214-223.

Goossens, H., de Leeuw, J.W., Schenck, P.A. and Brassell, S.C., 1984. Tocopherols as likely precursors of pristane in ancient sediments and crude oils. Nature, 312, 440-442.

Grantham P.J. and Wakefield, L.L., 1988. Variations in the sterane carbon number distributions of marine source rock derived crude oils through geological times. Organic Geochemistry, 12, 61–77.

Gratzer, R., Sachsenhofer, R.F., Bechtel, A., Schulz, H.M. and Smuk, A., 2008. Oil-oil and Oil-source Rock Correlation in the Alpine Foreland Basin Austria. 70th EAGE Conference & Exhibition. Extended Abstract, P243.

Haq, B.U., Hardenbohl, J. and Vail, P.R., 1987. Chronology of fluctuating sea levels since the Triassic. Science, 235, 1156-1167.

ten Haven, H.L., de Leeuw, J.W., Rullkötter, J. and Sinninghe Damste, J.S., 1987. Restricted utility of the pristane / phytane ratio as a palaeoenvironmental indicator. Nature, 330, 641-643.

Head, M.J., Seidenkrantz, M.-S., Janczyk-Kopikowa, Z., Marks, L. and Gibbard, P.L., 2005. Last Interglacial (Eemian) hydrographic conditions in the southeastern Baltic Sea, NE Europe, based on dinoflagellate cysts. Quaternary International, 130, 3-30.

Hubbard, S.M., De Ruig, M.J. and Graham, S.A., 2005. Utilizing outcrop analogs to improve subsurface mapping of natural gas-bearing strata in the Puchkirchen Formation, Molasse Basin, Upper Austria. Austrian Journal of Earth Sciences, 98, 52-66.

Islam, M.A., 1984. A study of Early Eocene palaeoenvironments in the Isle of Sheppey as determined from microplankton assemblage composition. Tertiary Research, 6, 11-21.

Jin, J., Aigner, T., Luterbacher, H.P., Bachmann, G.H. and Müller, M., 1995. Sequence stratigraphy and depositional history in the south-eastern German Molasse Basin. Marine and Petroleum Geology, 12, 929-940.

Köthe, A., 1990. Paleogene Dinoflagellates from Northwest Germany – Biostratigraphy and Paleoenvironment. Geologisches Jahrbuch, A118, 3-111.

Krhovský, J. and Djurasinovic, M., 1993. The nannofossil chalk layers in the early Oligocene Sitborice Member in Velké Nemcice (the Menilitic formation, Zdánice Unit, South Moravia): Orbitally forced changes in paleoproductivity. In: B. Hamrsmid (ed.), Nové výsledky v terciéru západních Karpat. Sbornik referatu z 10. konference o mladším terciéru, Brno, 27.-28.4.1992, Knihovnicka Zemni Plyn Nafta, Hodonin, 15, 33-53.

Langford, F.F. and Blanc-Valleron, M.-M., 1990. Interpreting Rock-Eval pyrolysis data using graphs of pyrolyzable hydrocarbons vs. total organic carbon. American Association of Petroleum Geologists Bulletin, 74, 799-804.

Mackenzie, A.S., 1984. Application of biological markers in petroleum geochemistry. In: D. Welte and J. Brooks (eds.), Advances in Petroleum Geochemistry, 1, 115-214.

Martini, E., 1971. Standard Tertiary and Quaternary calcareous nannoplankton zonation. In: A. Farinacci (ed.), Proceedings of the II Planktonic Conference. Edizioni Tecnoscienza, Roma, 739-785.

Melinte, M.C., 2005. Oligocene paleoenvironmental changes in the Romanian Carpathians, revealed by calcareous nannofossils. Studia Geologica Polonica, 124, 341-352.

Müller, C., 1970. Nannoplankton-Zonen der Unteren Meeresmolasse Bayerns. Geologica Bavarica, 63, 107-117.

Nagymarosy, A., 1991. The response of the calcareous nannoplankton to the Early Oligocene separation of the Paratethys. 4th International Nannoplankton Association Conference Abstracts, Prague 1991, INA Newsletter 13, 62-63.

Ourisson, G., Albrecht, P. and Rohmer, M., 1979. The hopanoids: palaeo-chemistry and biochemistry of a group of natural products. Pure Applied Chemistry, 51, 709-729.

Peters, K.E., 1986. Guidlines for Evaluating Petroleum Source Rock Using Programmend Pyrolysis. American Association of Petroleum Geologists Bulletin, 70, 318-329.

Peters, K.E., Walters, C.C. and Moldowan, J.M., 2005. The Biomarker Guide. Vol. 2: Biomarkers and isotopes in petroleum exploration and earth history. Cambridge University Press, Cambridge, pp. 475-1155.

Picha, F.J. and Stranik, Z., 1999. Late Cretaceous to early Miocene deposits of the Carpathian foreland basin in southern Moravia. International Journal Earth Sciences, 88, 475-495.

Pittet, B. and Gorin, G.E., 1997. Distribution of sedimentary organic matter in a mixed carbonate-siliciclastic platform environment: Oxfordian of the Swiss Jura Mountains. Sedimentology, 44, 915-937.

Rasser, M.W. and Piller, W.E., 2004. Crustose algal frameworks from the Eocene Alpine Foreland. Paleogeography, Paleoclimatology, Paleoecology, 206, 21-39.

Rögl, F., Hochuli, P. and Müller, C., 1979. Oligocene–Early Miocene stratigraphic correlations in the Molasse Basin of Austria. Annales Geologiques des Pays Helleniques Tome hors series, 1045-1050.

Röhl, H.-J., Schmid-Röhl, A., Oschmann, W., Frimmel, A. and Schwark, L., 2001. The Posidonia Shale (Lower Toarcian) of SW-Germany: an oxygen-depleted ecosystem controlled by sea level and palaeoclimate. Palaeogeography, Palaeoclimatology, Palaeoecology, 165, 27-52.

Rohmer, M., Bisseret, P. and Neunlist, S., 1992. The hopanoids, prokaryotic triterpenoids and precursors of ubiquitous molecular fossils. In: J.M. Moldowan, P. Albrecht and R.P. Philp (eds.), Biological Markers in Sediments and Petroleum, Prentice Hall, Englewood Cliffs, N.J., pp. 1-17.

Sachsenhofer, R.F. and Schulz, H.-M., 2006. Architecture of Lower Oligocene source rocks in the Alpine Foreland Basin: a model for syn- and post-depositional source-rock features in the Paratethyan realm. Petroleum Geoscience, 12, 363-377.

Sachsenhofer, R.F., Stummer, B., Georgiev, G., Dellmour, R., Bechtel, A., Gratzer, R. and Ćorić, S., 2009. Depositional environment and hydrocarbon source potential of the Oligocene Ruslar Formation (Kamchia Depression; Western Black Sea). Marine and Petroleum Geology, 26, 57-84.

Schmidt, F. and Erdogan, L. T., 1996. Palaeohydrodynamics in exploration. In: G. Wessely and W. Liebl (eds.) Oil and Gas in Alpidic Thrustbelts and Basins of Central and Eastern Europe. European Association of Geoscientists and Engineers Special Publication, 5, The Alden Press, Oxford, 255-265.

Schulz H.-M., Sachsenhofer, R. F., Bechtel, A., Polesny, H. and Wagner, L., 2002. The origin of hydrocarbon source rocks in the Austrian Molasse Basin (Eocene-Oligocene transition). Marine and Petroleum Geology, 19, 683-709.

Schulz H.-M., Bechtel, A., Rainer, T., Sachsenhofer, R.F. and Struck, U., 2004. Paleocenaography of the western Central Paratethys during nannoplankton zone NP 23: The Dynow Marlstone in the Austrian Molasse Basin. Geologica Carpathica, 55, 311-323.

Schulz, H.-M., Bechtel, A. and Sachsenhofer, R.F., 2005. The birth of the Paratethys during the early Oligocene: from Tethys to an ancient Black Sea analogue? Global and Planetary Change, 49, 163-176.

Seifert, W.K. and Moldowan, J.M., 1986. Use of biological markers in petroleum exploration, In: R.B. Johns (ed.), Methods in Geochemistry and Geophysics, 24, 261-290.

Sinninghe Damsté, J.S. Kelly, B. Betts, S. Baas, M. Maxwell J.R. and de Leeuw, J.W., 1993. Variations in abundances and distributions of isoprenoid chromans and long chain alkylbenzenes in sediments of the Mulhouse Basin: A molecular sedimentary record of paleosalinity. Organic Geochemistry, 20, 1201-1215.

Sissingh, W., 1997. Tectonostratigraphy of the North Alpine Foreland Basin: correlation of Tertiary depositional cycles and orogenic phases. Tectonophysics, 282, 223-256.

Švábenická, L., 1999. Braarudosphaera-rich sediments in the Turonian of the Bohemian Cretaceous Basin, Czech Republic. Cretaceous Research, 20, 773-782.

Talbot, M. R., 1990. A review of the palaeohydrological interpretation of carbon and oxygen ratios in primary lacustrine carbonates. Chemical Geology, 80, 261-279.

Tissot, B.T. and Welte, D.H., 1984. Petroleum Formation and Occurrences. 2nd Edition, Springer Verlag, Berlin, 699 pp.

Torricelli, S. and Biffi, U., 2001. Palynostratigraphy of the Numidian Flysch of northern Tunisia (Oligocene–Early Miocene). Palynology, 25, 29-55.

Tyson, R.V., 1995. Sedimentary Organic Matter. Organic facies and palynofacies. Chapman & Hall, London, 615 pp.

Van Simaeys, S., Munsterman, D., Brinkhuis, H., 2005. Oligocene dinoflagellate cyst biostratigraphy of the southern North Sea Basin. Review of Palaeobotany and Palynology, 134, 105-128.

Volkman, J.K., 1986. A review of sterol markers for marine and terrigenous organic matter. Organic Geochemistry, 9, 83-99.

Volkman, J.K. and Maxwell, J.R., 1986. Acyclic isoprenoids as biological markers. In: R.B. Johns (ed.), Biological Markers in the Sedimentary Record. Elsevier, Amsterdam, pp. 1-42.

Wagner, L.R., 1996. Stratigraphy and hydrocarbons in Upper Austrian Molasse Foredeep (active margin). In: G. Wessely and W. Liebl (eds.) Oil and Gas in Alpidic Thrustbelts and Basins of Central and Eastern Europe. European Association of Geoscientists and Engineers Special Publication, 5, The Alden Press, Oxford, 217-235.

Wagner, L.R., 1998. Tectono-stratigraphy and hydrocarbons in the Molasse Foredeep of Salzburg, Upper and Lower Austria. In: A. Mascle, C. Puigdefàbregas and H.P. Luterbacher (eds.) Cenozoic Foreland Basins of Western Europe. Geological Society London Special Publications, 134, 339-369.

Wagner, L., Kuckelkorn, K. and Hiltmann, W., 1986. Neue Ergebnisse zur alpinen Gebirgsbildung Oberösterreichs aus der Bohrung Oberhofen 1 – Stratigraphie, Fazies, Maturität und Tektonik. Erdöl, Erdgas, Kohle, 102, 12-19.

Williams, G.L., Brinkhuis, H., Pearce, M.A, Fensome, R.A. and Weegink, J.W., 2004. Southern Ocean and global dinoflagellate cyst events compared; Index events for the Late Cretaceous-Neogene. In: N.F. Exon, J.P. Kennett and M.J. Malone (eds.) Proceedings of the Ocean Drilling Program, Scientific Results ODP Leg 189, 1-98.

Wilpshaar, M., Santarelli, A., Brinkhuis, H. and Visscher, H., 1996. Dinoflagellate cysts and mid-Oligocene chronostratigraphy in the central Mediterranean region. Journal of the Geological Society of London, 153, 553-561.

Zweigel, J., 1998. Eustatic versus tectonic control on foreland basin fill. Contributions to Sedimentary Geology, 20, 1-140.

Reinhard F. SACHSENHOFER[1),*)], Birgit LEITNER[1)], Hans-Gert LINZER[2)], Achim BECHTEL[1)], Stjepan ĆORIĆ[3)], Reinhard GRATZER[1)], Doris REISCHENBACHER[1)] & Ali SOLIMAN[4)]

[1)] Department Applied Geosciences and Geophysics, Montanuniversität, Peter-Tunner-Str. 5, A-8700 Leoben, Austria;

[2)] Rohöl-Aufsuchungs AG, Schwarzenbergplatz 16, A-1015 Vienna, Austria;

[3)] Geological Survey of Austria, Neulinggasse 38, A-1030 Vienna, Austria;

[4)] Institute of Earth Sciences, Karl-Franzens-Universität Graz, Heinrichstr. 26, A-8010 Graz, Austria;

[*)] Corresponding author, reinhard.sachsenhofer@unileoben.ac.at

Plate 1:

Scale bar = 20 µm

Figure	**1:**	*Wetzeliella gochtii* Costa and Downie, 1976; well Egdg; sample 77; slide C, England Finder P39/1; dorsal view.
Figure	**2, 3:**	*Wetzeliella articulata* Eisenack, 1938; well Egdg; sample 77; slide C, England Finder T32; different foci.
Figure	**4:**	*Fibrocysta axialis* (Eisenack, 1965) Stover and Evitt, 1978; well Osch; sample 62; slide E; England Finder T45/1; dorsal view.
Figure	**5:**	*Glaphyrocysta texta* (Bujak, 1976) Stover and Evitt, 1978; well Egdg; sample 77; slide X, England Finder V66/2; ventral view.
Figure	**6:**	*Distatodinium scariosum* Liengjarern et al., 1980; well Egdg; sample 77; slide C, England Finder L43/4; ?dorsal view.
Figure	**7, 11:**	*Distatodinium ellipticum* (Cookson, 1965) Eaton, 1976; well Egdg; sample 77; slide C, England Finder D53/1; different foci.
Figure	**8, 9:**	*Hystrichokolpoma truncatum* Biffi and Manum, 1988; well Egdg; sample 83; slide X, England Finder B38/1; dorsal view; different foci.
Figure	**10:**	*Enneadocysta pectiniformis* (Gerlach, 1961) emend. Stover and Williams, 1995; well Egdg; sample 77; slide C; uncertain view.
Figure	**12, 13:**	*Deflandrea phosphoritica* Eisenack, 1938; well Osch; sample 67; slide X; England Finder D32; dorsal view; different foci.
Figure	**14, 15:**	*Cordosphaeridium cantharellus* (Brosius, 1963) Gocht, 1969; well Egdg; sample 83; slide X, England Finder H60; different foci.
Figure	**16:**	*Selenopemphix armata* Bujak in Bujak et al., 1980; well Egdg; sample 77; slide C; England Finder M59; antapical view.
Figure	**17:**	*Selenopemphix nephroides* Benedek, 1972; emend. Benedek and Sarjeant, 1981; well Osch; sample 62; slide E; England Finder T62; ?antapical view.
Figure	**18:**	*Lejeunecysta fallax* (Morgenroth, 1966) Artzner and Dörhöfer, 1978; emend. Biffi and Grignani, 1983; well Egdg; sample 77; slide C; England Finder V60; dorsal view.
Figure	**19:**	*Distatodinium biffii* Brinkhuis et al., 1992; well P; slide C, England Finder P27/3; uncertain view.